Study on the intestinal absorption of oligopeptides by electrospray ionization-mass spectrometric assay

申, 偉琳

出版情報：Kyushu University, 2021, 博士（農学）, 課程博士
バージョン：
権利関係：

Study on the intestinal absorption of oligopeptides by electrospray ionization-mass spectrometric assay

Weilin Shen

Kyushu University

2022

LIST OF CONTENTS

Abbreviations

- ACE, angiotensin converting enzyme
- ACN, acetonitrile
- ADME, absorption, distribution, metabolism, excretion
- AGEs, advanced glycation end-products
- APDS, 3-aminopyridyl-*N*-hydroxysuccinimidyl carbamate
- B.W., body weight
- Cbl-b, Casitas B-cell lineage lymphoma-b
- Cblin peptides, Cbl-b inhibitory peptides
- CMA, Connolly molecular area
- Cou, *N*-succinimidyl 7-methoxycoumarin-3-carboxylate
- CV, coefficient of variance
- DMEM, Dulbecco's modified Eagle's medium
- DPP-IV, dipeptidyl peptidase IV
- EIC, extracted ion chromatogram
- ESI, electrospray ionization
- FA, formic acid
- FBS, fetal bovine serum
- FFC, Foods with Functional Claims
- FOSHU, Foods for Specified Health Uses
- HBSS, Hank's balanced salt solution
- HEPES, *N*-2-hydroxyethylpiperazine-*N*'-2-ethanesulfonic acid
- HPLC, high performance liquid chromatography
- IGF-1, insulin-like growth factor-1
- IRS-1, insulin receptor substrate-1
- LOD, limit of detection
- MeOH, methanol
- MES, 2-(*N*-morpholino)ethanesulfonic acid
- MS, mass spectrometry
- NDA, naphatalene-2,3-dialdehyde
- P_{app}, apparent permeability coefficient
- *S/N*, signal-to-noise ratio
- SD rat, Sprague-Dawley rat
- SEM, standard error of the mean
- SHR, spontaneously hypertensive rats
- TEER, transepithelial electrical resistance
- TJ, tight junction
- TNBS, trinitrobenzene sulfonate
- TNP, trinitrophenyl
- UV/Vis, ultraviolet/visible

Chapter I

Introduction

Peptides are usually derived from food protein sources, either during food processing procedures such as chemical/enzymatic hydrolysis, microbial fermentation, etc., or through gastric-intestinal degradation upon oral intake. A large variety of bioactive peptides with various chain lengths and amino acid compositions have been identified and extensively studied *in vitro* and *in vivo* over the past several decades [1]. Most bioactive peptides are usually composed of 2 – 20 amino acids, and are thought to be able to prevent the onset of some life-style related diseases including cardiovascular diseases, diabetes, hyperlipidemia, etc. [1]. In Japan, many food products containing bioactive peptides have been approved as Foods for Specified Health Uses (FOSHU) and Foods with Functional Claims (FFC) by the Consumers Affair Agency for daily usage [2, 3]. Typical FOSHU and FFC peptides are listed in Table 1-1.

Table 1-1. Peptide ingredients approved as FOSHU/FFC products.

Peptide sequence	Source	Bioactivity	
VY	Sardine, royal jelly, seaweed	Anti-hypertensive	FOSHU/FFC
IY	Royal jelly, seaweed	Anti-hypertensive	FOSHU/FFC
FY	Seaweed	Anti-hypertensive	FFC
VPP	Milk	Anti-hypertensive	FOSHU/FFC
IPP	Milk	Anti-hypertensive	FOSHU/FFC
LVY	Sesame	Anti-hypertensive	FOSHU
IVY	Royal jelly	Anti-hypertensive	FOSHU
MKP	Milk	Anti-hypertensive	FFC
AKYSY	Seaweed	Anti-hypertensive	FOSHU
NIPPLTQTPVVVPPFLQPE	Milk	Cognitive function	FFC

(Source: https://www.caa.go.jp)

To clarify the peptide-induced bioactivities and ultimately health-promoting effects in human, absorption, distribution, metabolism, and excretion (ADME) analysis is of vital importance (Figure 1-1) [4]. To elicit health-claimed bioactivities, peptides must reach their target organs in the body. The small intestinal barrier, lined by intestinal epithelial cells, separates the external environments and internal milieu, and serves as a pathway responsible for nutrient absorption [5]. Therefore, upon oral intake, crossing of peptides beyond the intestinal barrier is required to eventually reach targeted tissues or organs via blood circulation.

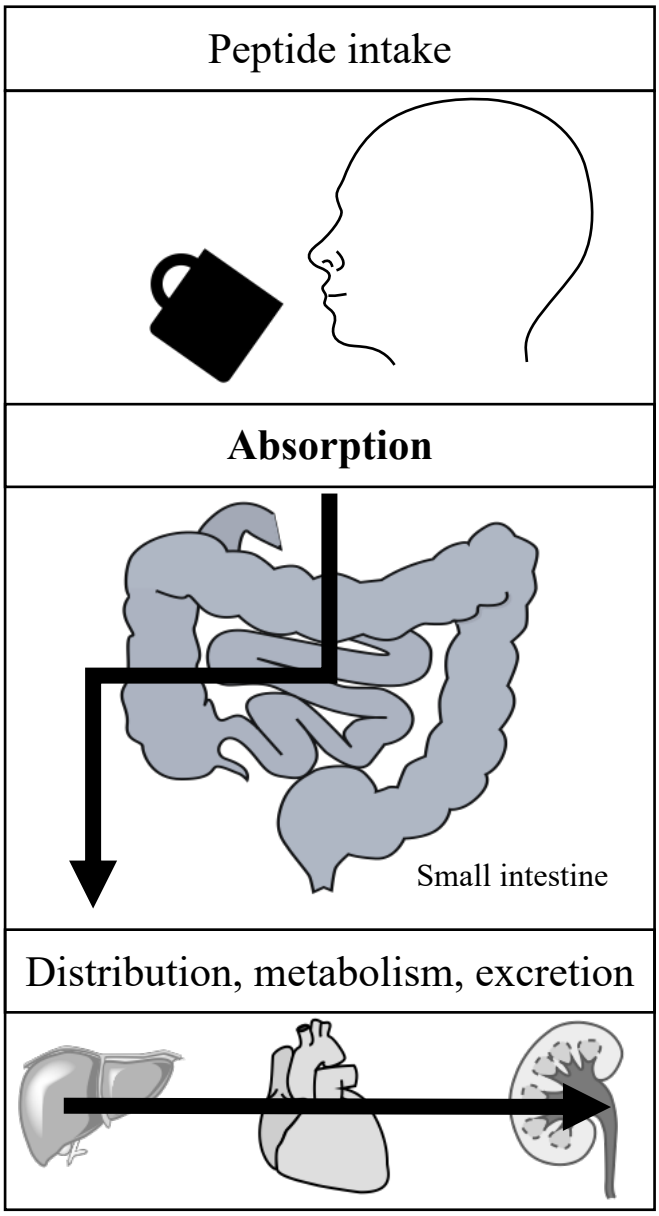

Figure 1-1. Scheme of peptide absorption, distribution, metabolism, and excretion (ADME) upon oral intake in mammals.

A proton-coupled transporter of oligopeptides was cloned and functionally characterized in 1994 from rabbit small intestine [6], and was later identified also in mouse and human [7, 8]. Named PepT1, the transporter exhibited broad specificity for di-/tripeptides and peptidomimetic drugs [6]. An anti-hypertensive dipeptide VY identified from sardine muscle hydrolysate was demonstrated to be absorbed via PepT1 using jejunal membranes of spontaneously hypertensive rats (SHRs) [9]. Oral intake of the peptide in mild hypertensive subjects at a dose of 12 mg resulted in an elevated concentration in blood circulation to a maximum of 2,041 ± 148 fmol/mL-plasma [10]. Furthermore, in a randomized double-blind placebo-controlled clinical trial involving 29 volunteers, VY at a dose of 3 mg, twice a day, significantly reduced the systolic and diastolic blood pressures by 9.3 and 5.2 mmHg at 4 weeks [11]. These studies demonstrated for the first time that small peptides could be absorbed and play a role in health promotion in humans. Meanwhile, VPP and IPP derived from fermented milk are other examples of extensively studied bioactive peptides in human subjects [1, 12]. A recent meta-analysis summarizing 33 sets of clinical data regarding VPP and IPP demonstrated that the two lactotripeptides could potentially lower blood pressure, especially in Asian population [13]. Although VPP and IPP can be recognized by PepT1, VPP and IPP incorporated into cells by PepT1 were susceptible to intracellular degradation and thus could not reach blood circulation [14]. Instead, in contrast to VY, these lactotripeptides have been demonstrated to be absorbed by passive diffusion via paracellular tight junction (TJ) [14]. Nonetheless, the

peptides still could be absorbed upon oral intake at sub-pmol/mL plasma levels in human subjects [15]. Besides sardine peptide VY and lactotripeptides VPP and IPP, few bioactive peptides have undergone clinical studies. Instead, Caco-2 cells derived from human colonic adenocarcinoma have been characterized and used as an intestinal epithelial cell model to study *in vitro* transport behavior of small peptides [16–18]. Caco-2 cells differentiate and form monolayers that morphologically and functionally resemble mature enterocytes, expressing diverse digestive enzymes including proteases and peptidases, membrane transporters including PepT1, and TJ-related proteins between cells [17, 18]. Caco-2 cell studies revealed that active transport via PepT1 and passive diffusion via paracellular TJ are commonly responsible for the transport of di-/tripeptides in the small intestine (Figure 1-2) [19]. A list of Caco-2 transportable di-/tripeptides are shown in Table 2.

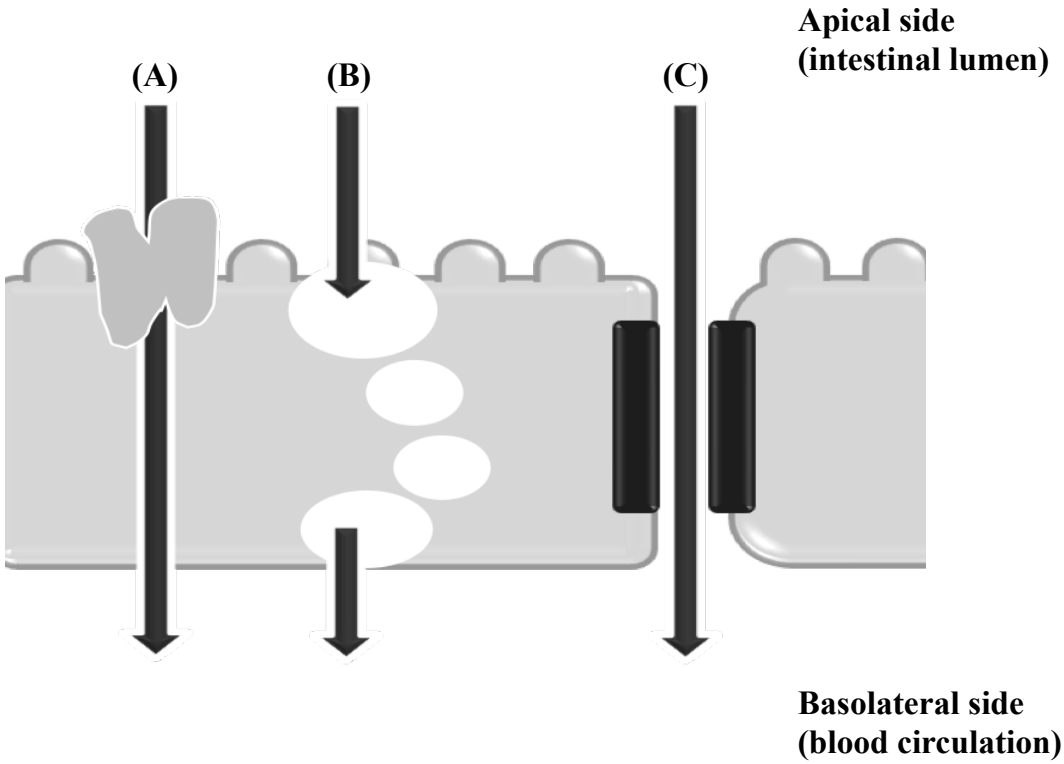

Figure 1-2. Scheme of peptide transport routes across Caco-2 cell monolayers. (A) PepT1-mediated transport, (B) Transcytosis, (C) Passive diffusion via paracellular TJ.

Table 1-2. Caco-2 transportable di-/tripeptides, their bioactivity, P_{app}, and transport routes.

Residues	Sequence	Bioactivity	P_{app} (cm/s)	Transport route	Ref	Year
2	AF	ACE inhibitory	1.4×10^{-6}	PepT1	[20]	2008
2	FI	ACE inhibitory	1.4×10^{-6}	PepT1	[20]	2008
2	IF	ACE inhibitory	2.4×10^{-6}	PepT1	[20]	2008
2	AW	ACE inhibitory	*na*	*na*	[21]	2008
2	VF	ACE inhibitory	*na*	*na*	[21]	2008
2	VY	ACE inhibitory	*na*	*na*	[21]	2008
2	VY	Anti-hypertensive	6.8×10^{-6}	PepT1	[22]	2013
2	IF	ACE inhibitory	2.9×10^{-6}	PepT1	[22]	2013
2	WQ	Anti-hypertensive	3.9×10^{-8}	TJ	[23]	2013
2	WH	Anti-hypertensive	8.1×10^{-6}	*na*	[24]	2015
2	HW	Anti-hypertensive	4.6×10^{-6}	*na*	[24]	2015
2	YL	Satiating	3.3×10^{-6}	*na*	[25]	2014
2	PO	Diverse bioactivity	1.3×10^{-7}	*na*	[26]	2016
2	LY	ACE and renin inhibitory	3.5×10^{-6}	*na*	[27]	2017
2	TF	ACE and renin inhibitory	9.4×10^{-7}	*na*	[27]	2017
2	WR	DPP-IV inhibitory	*na*	*na*	[28]	2017
2	YV	ACE inhibitory	*na*	*na*	[29]	2018
2	IW	ACE inhibitory/anti-inflammatory/antioxidative	2.0×10^{-7}	PepT1	[30]	2018
3	VPP	ACE inhibitory	*na*	TJ	[14]	2002

Table 1-2. Continued.

Residues	Sequence	Bioactivity	P_{app} (cm/s)	Transport route	Ref	Year
3	VPP	ACE inhibitory	0.5×10^{-8}	TJ	[31]	2008
3	IPP	ACE inhibitory	1.0×10^{-8}	TJ	[31]	2008
3	YPI	Anti-hypertensive	*na*	PepT1	[32]	2008
3	VPY	Anti-inflammatory	*na*	PepT1	[33]	2012
3	IRW	Anti-hypertensive	*na*	PepT1/TJ	[34]	2013
3	RWQ	Anti-hypertensive	0.7×10^{-8}	TJ	[23]	2013
3	GPO	Diverse bioactivity	1.1×10^{-6}	*na*	[26]	2016
3	IPI	DPP-IV inhibitory	*na*	*na*	[28]	2017
3	IPP	ACE inhibitory	6.8×10^{-6}	PepT1/TJ	[35]	2017
3	LKP	Antihypertensive	8.9×10^{-6}	PepT1/TJ	[35]	2017
3	LSW	Antihypertensive	1.2×10^{-7}	PepT1/TJ	[36]	2017
3	LKP	ACE inhibitory	1.8×10^{-7}	PepT1/TJ	[37]	2017
3	IQW	ACE inhibitory	1.3×10^{-7}	PepT1/TJ	[37]	2017
3	IWH	ACE inhibitory/anti-inflammatory/antioxidative	3.8×10^{-7}	PepT1/TJ	[30]	2018
3	LLY	Anti-hypertensive/anti-oxidative	*na*	PepT1	[38]	2018
3	IQP	ACE inhibitory	7.5×10^{-6}	TJ	[39]	2018
3	VEP	ACE inhibitory	5.1×10^{-6}	TJ	[39]	2018
3	GPR	Anti-platelet aggregative	*na*	*na*	[40]	2020

ACE, angiotensin converting enzyme
na, not available

In addition to di-/tripeptides, longer bioactive oligopeptides could also penetrate Caco-2 cell monolayers. There are 66 bioactive peptides ranging from 4 to 43 amino acid chain lengths that are reported in 44 transport studies since 1997 (30 since 2016, Table 1-3). Compared to di-/tripeptides, longer oligopeptides showed more diverse bioactivities, including anti-oxidative, angiotensin converting enzyme (ACE)-inhibitory, dipeptidyl peptidase IV (DPP-IV)-inhibitory, hypocholesterolemic, osteogenic, satiating, immunomodulatory effects, etc. Passive diffusion via paracellular TJ was reported to be the major transport route, while a few could enter the cell and be transported by transcellular transcytosis (Figure 1-2). The reported apparent permeability coefficient (P_{app}), which has been applied to evaluate the transport velocity of peptides across Caco-2 cell monolayers, varied by two orders of magnitude depending on the sequences.

Table 1-3. Caco-2 transportable oligopeptides, their bioactivity, P_{app}, and transport routes.

Residues	Sequence	Bioactivity	P_{app} (cm/s)	Transport route	Ref	Year
4	GGYR	Papain inhibitory	*na*	TJ	[41]	1997
4	PFGK	*na*	*na*	*na*	[41]	1997
4	VGPV	ACE inhibitory	*na*	TJ	[42]	2016
4	AHLL	ACE inhibitory	2.64×10^{-6}	TJ/transcellular	[43]	2017
4	RALP	ACE and renin inhibitory	0.32×10^{-6}	*na*	[27]	2017
4	DLEE	Anti-oxidative	3.32×10^{-6}	TJ	[44]	2018
4	KPLL	ACE inhibitory	*na*	TJ	[45]	2018
4	LPYP	Hypocholesterolemic	*na*	*na*	[46]	2018
4	GPRG	Anti-platelet aggregative	*na*	*na*	[40]	2020
4	YLNF	DPP-IV inhibitory	3.54×10^{-6}	*na*	[47]	2021
5	YPFPG	ACE inhibitory	*na*	*na*	[41]	1997
5	HLPLP	ACE inhibitory	*na*	TJ	[48]	2008
5	VLPVP	ACE inhibitory	0.74×10^{-7}	TJ	[49]	2008
5	YAEER	Anti-hypertensive	*na*	*na*	[32]	2008
5	YPFPG	μ-Opioid receptor agonist	0.17×10^{-5}	*na*	[50]	2009
5	QIGLF	ACE inhibitory	9.11×10^{-7}	TJ	[51]	2014
5	RVPSL	Anti-hypertensive	6.97×10^{-6}	TJ	[52]	2015
5	GPRGF	ACE inhibitory	*na*	TJ	[42]	2016

Table 1-3. Continued.

Residues	Sequence	Bioactivity	P_{app} (cm/s)	Transport route	Ref	Year
5	GYYPT	Opioid	*na*	TJ	[53]	2016
5	YPISL	Opioid	*na*	TJ	[53]	2016
5	LPYPY	DPP-IV inhibitory	*na*	*na*	[28]	2017
5	IPIQY	DPP-IV inhibitory	*na*	*na*	[28]	2017
5	IWHHT	ACE inhibitory/anti-inflammatory/antioxidative	2.20×10^{-7}	TJ	[30]	2018
5	YFCLT	Antioxidative	1.10×10^{-7}	TJ/transcytosis	[54]	2018
5	ELFTT	ACE inhibitory	*na*	*na*	[45]	2018
5	GPRGP	Anti-platelet aggregative	*na*	*na*	[40]	2020
6	SRYPSY	μ-Opoid receptor agonist	1.54×10^{-5}	*na*	[50]	2009
6	KVLPLP	ACE inhibitory	2.78×10^{-7}	TJ	[55]	2009
6	KPVAAP	ACE inhibitory	*na*	*na*	[56]	2016
6	TNGIIR	ACE inhibitory	4.92×10^{-6}	TJ	[57]	2016
6	RLSFNP	ACE inhibitory	*na*	TJ	[58]	2018
6	KPLLCS	ACE inhibitory	*na*	*na*	[45]	2018
6	IADHFL	DPP-IV inhibitory	4.91×10^{-8}	TJ	[59]	2018
6	LSGYGP	ACE inhibitory	*na*	*na*	[60]	2019
6	RLSFNP	ACE inhibitory	8.27×10^{-7}	Transcytosis	[61]	2019
6	YFYPQL	Anti-oxidative/anti-inflammatory	0.79×10^{-6}	Transcytosis	[62]	2019

Table 1-3. Continued.

Residues	Sequence	Bioactivity	P_{app} (cm/s)	Transport route	Ref	Year
6	WGAPSL	Hypocholesterolemic	4.4×10^{-8}	TJ	[63]	2019
6	KYIPIQ	ACE inhibitory	*na*	TJ	[64]	2020
6	IPGSPY	DPP-IV inhibitory	*na*	*na*	[65]	2020
6	LVLPGE	ACE inhibitory	5.09×10^{-7}	PepT1/TJ	[66]	2021
7	ALPMHIR	ACE inhibitory	*na*	*na*	[67]	2002
7	YPFPGPI	μ-Opioid receptor antagonist	0.17×10^{-5}	*na*	[50]	2009
7	YLGYLEN	Anxiolytic	0.65×10^{-6}	*na*	[68]	2011
7	YPFPGPI	Satiating	0.13×10^{-6}	*na*	[25]	2014
7	VLPVPQK	Anti-oxidative/ACE inhibitory	*na*	PepT1/SOPT2	[69]	2016
7	TKLPAVF	DPP-IV inhibitory	1.46×10^{-6}	*na*	[47]	2021
7	LDKVFER	DPP-IV inhibitory	4.23×10^{-7}	TJ	[70]	2021
8	FRADHPFL	Anxiolytic	*na*	*na*	[41]	1997
8	FRADHPFL	ACE inhibitory	*na*	*na*	[32]	2008
8	GAOGLOGP	ACE inhibitory	1.99×10^{-7}	TJ	[71]	2010
8	RKQLQGVN	Chemopreventive	2.50×10^{-7}	TJ	[72]	2018
8	IAVPGEVA	Hypocholesterolemic	*na*	*na*	[46]	2018
8	IAVPTGVA	Hypocholesterolemic	*na*	*na*	[46]	2018
8	QAGLSPVR	ACE inhibitory	*na*	TJ	[73]	2019

Table 1-3. Continued.

Residues	Sequence	Bioactivity	P_{app} (cm/s)	Transport route	Ref	Year
8	ELHQEQPL	DPP-IV inhibitory	0.45×10^{-6}	TJ	[74]	2020
8	VLATSGPG	DPP-IV inhibitory	2.41×10^{-7}	TJ/transcytosis	[70]	2021
8	LPKHSDAD	Hypocholesterolemic	*na*	TJ	[75]	2021
9	LKPTPEGDL	DPP-IV inhibitory	*na*	*na*	[28]	2017
9	WDHHAPQL	Anti-oxidative	0.82×10^{-6}	TJ	[76]	2018
10	YLGYLENLLR	Anxiolytic	*na*	*na*	[68]	2011
10	YWDHNNPQIR	Anti-oxidative	0.66×10^{-6}	Transcytosis	[77]	2017
10	LILPKHSDAD	Hypocholesterolemic	*na*	TJ	[75]	2021
12	WGDEHLPGSPYH	DPP-IV inhibitory	*na*	*na*	[65]	2020
12	LEELEEELEAER	Osteogenic	1.16×10^{-5}	*na*	[78]	2020
17	β-casein (193 – 209)	Immunomodulatory	*na*	TJ/transcytosis	[79]	2010
43	Lunasin	Chemopreventive	3.32×10^{-7}	TJ	[72]	2017

na, not available.

Nonetheless, it should be noted that Caco-2 transport behavior may not reflect the actual *in vivo* absorption of a peptide. For instance, while WH was absorbed into rat blood circulation upon oral administration, its reverse sequence HW was not absorbable due to *in vivo* enzymatic degradation by aminopeptidases or endopeptidases specifically recognizing *C*-terminal tryptophan during the absorption process, despite that the P_{app} of WH and HW were comparable [24]. Therefore, Caco-2 cell studies alone may not be adequate to evaluate the absorption of oligopeptides, i.e., to exploit the potential diverse bioactivities of oligopeptides in health promotion, both *in vitro* studies using Caco-2 monolayers and *in vivo* studies using animal models are essential to understand the intestinal absorption behavior. In contrast to extensive Caco-2 cell studies, the *in vivo* absorption behavior of oligopeptides still needs to be clarified.

To elucidate the intestinal absorption behavior of oligopeptides, reliable detection assay systems are crucial. Conventionally, high performance liquid chromatograph (HPLC) coupled to ultraviolet-visible spectrophotometer (UV/Vis) has been used in peptide analysis. The HPLC-UV/Vis method enabled quantification of peptides at μM level and has been widely used as a quantitative method in Caco-2 studies [19]. The understanding on the *in vivo* absorption of bioactive peptides was greatly

advanced by the emergence of electrospray ionization mass spectrometry (ESI-MS), a technique that largely improved the detection specificity and sensitivity of small peptides [80]. Moreover, chemical derivatizations furtherly enhanced MS signal intensity of small peptides. An amino group derivatization reagent, 2,4,6-trinitrobenzene sulfonate (TNBS), has been characterized and applied to enhance ESI-MS detection of dipeptides [81, 82]. The trinitrophenyl (TNP) moiety induced a 3 – 55 fold improvement in signal-to-noise ratio (*S/N*) and enabled detection of the targeted dipeptides at pM level [82]. The TNBS derivatization-aided LC-MS method was successfully applied to evaluate the absorption behavior of an anti-atherosclerotic dipeptide WH in Sprague-Dawley (SD) rats upon oral administration [24]. Currently, the ESI-MS detection characterization of longer oligopeptides with chemical derivatizations needs to be evaluated.

Recently, Nikawa and colleagues discovered a novel pentapeptide DG-phosphorylated (p)YMP which could ameliorate disuse muscle atrophy in animals [83–85]. Disuse muscle atrophy refers to a loss in body muscle mass caused by inactiveness of muscles, i.e., when experiencing unloading stress such as bedridden and microgravity [86, 87]. In the ageing societies, disuse muscle atrophy is growing to be a serious social issue, while currently resistance training is the sole countermeasure against disuse muscle atrophy. However, resistance training is usually time

consuming and not applicable to the elderly due to physical restraints. Consequently, alternative approaches to prevent/treat disuse muscle atrophy through food or therapeutics are expected.

Nikawa and colleagues [88] investigated the molecular mechanisms of disuse muscle atrophy and reported that ubiquitin ligase Casitas B-cell lineage lymphoma-b (Cbl-b) plays a vital role in proteolysis under unloading conditions. Cbl-b binds with insulin receptor substrate 1 (IRS-1) and degrades this intracellular signaling molecule, blocking the insulin-like receptor 1 (IGF-1) pathway, resulting in an unbalance between protein synthesis and degradation [83]. Based on this mechanism, it was demonstrated that DGpYMP and DGYMP, corresponding to the 606 – 610 amino acids of IRS-1, could inhibit Cbl-b to elicit muscle atrophy preventive effects. Therefore, these peptides are named Cbl-b inhibitory peptides, i.e., Cblin in short [83] (Figure 1-3). In this study, the intestinal absorption behavior of Cblin peptides DGpYMP and DGYMP is thus targeted.

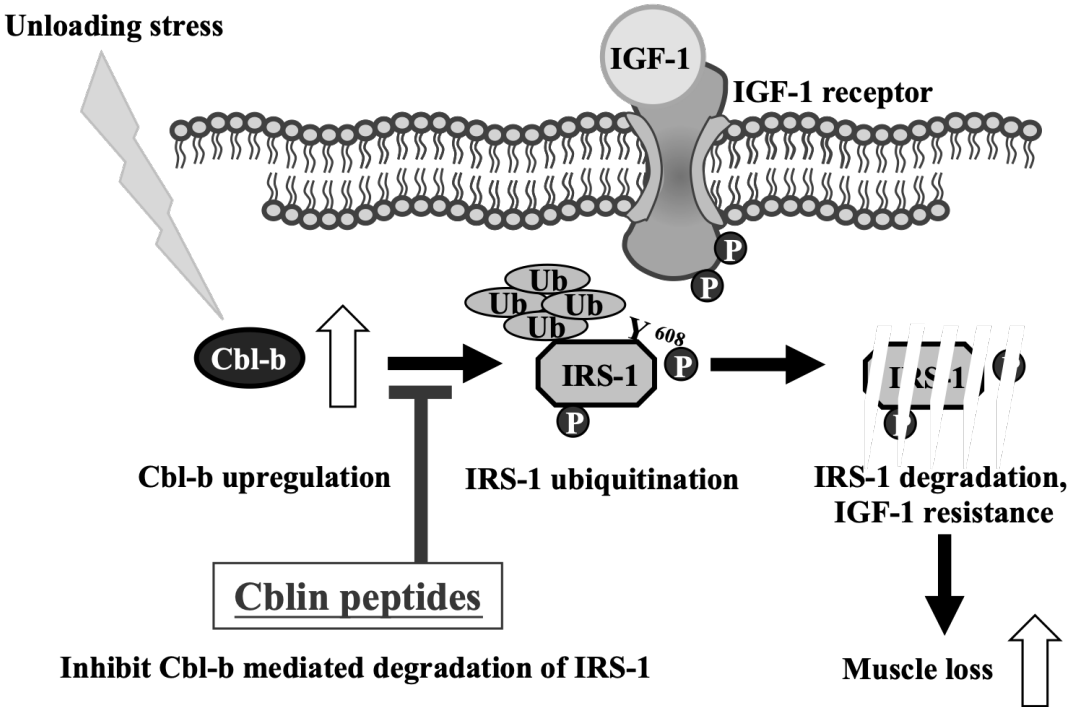

Figure 1-3. Cblin peptides in disuse muscle atrophy. Unloading stress upregulates ubiquitin ligase Cbl-b, which mediates degradation of IRS-1, leading to the resistance of IGF-1 signaling pathway, eventually results in muscle loss. Cblin peptides inhibit the function of Cbl-b to ameliorate disuse muscle atrophy.

According to the abovementioned background, oligopeptides with > 4 amino acid residues are growing to gain focus in the peptide science field, and the knowledge on the bioavailability is crucial to understand the potential bioactivity and health-promoting effect of oligopeptides in depth. Therefore, applying LC-ESI-MS as a quantitative approach, the aim of this study is to get insights on the intestinal absorption/metabolism of oligopeptides using Caco-2 cells *in vitro* and SD rats *in vivo*.

The objectives of each Chapter in this study are described as follows:

1) In **Chapter II**, as a highly sensitive assay to evaluate the intestinal absorption behavior of oligopeptides, the ESI-MS detection characteristics of oligopeptides were evaluated. A series of di- to penta- oligopeptides were chemically modified by four amino group derivatization reagents and were subjected to LC-ESI-time-of-flight (TOF)/MS analysis. The results indicated that for oligopeptides with > 4 amino acid residues, increasing hydrophobicity by chemical derivatization may not lead to enhanced detection sensitivity in contrast to di-/tripeptides, while the detection could be characterized by molecular surface area with an optimal of 250 – 300 $Å^2$.

2) In **Chapter III**, the intestinal absorption of muscle atrophy-preventive Cblin oligopeptides DGYMP and DGpYMP was investigated using Caco-2 cells and SD rats. LC-ESI-TOF/MS was applied for the highly sensitive quantitative analysis of the oligopeptides. It was demonstrated that the oligopeptides could be transported across Caco-2 cell monolayers, probably via paracellular tight junction. Moreover, in single oral administration experiments to SD rats, it was demonstrated that Cblin pentapeptide DGYMP could be absorbed into rat blood circulation in its intact peptide form, indicating that oligopeptides with > 4 amino acid residues could be absorbed upon oral intake, and potentially play a role in health promotion.

Chapter II

Characterization of electrospray ionization-mass spectrometric detection of oligopeptides

1. Introduction

Various bioactivities have been reported for small oligopeptides, including anti-hypertensive, anti-diabetic, anti-atherosclerotic, anti-inflammatory, anti-oxidative effects, etc. [1]. Taking the anti-hypertensive activity as an example, bioactive peptides have been reported (1) to modulate the metabolism of the renin-angiotensin system through the inhibition of angiotensin converting enzyme (ACE) in blood circulation and (2) to induce vascular relaxation through the inhibition of the voltage-dependent L-type Ca^{2+} channel in the aorta [89]. As such, it is considered that bioactive peptides may function through direct interaction with targeted tissues and organs; the *in vivo* functional appearance of such bioactive peptides upon oral intake requires them being absorbed into

blood circulation and being carried to targeted organs and tissues in intact peptide forms. The intestinal membrane is considered as the barrier separating the external and internal environments. Therefore, knowledge on bioavailability, especially absorption kinetics across the intestinal barrier, is essential to understand physiological functions of bioactive peptides.

The elucidation of intestinal absorption behavior of bioactive peptides relies on highly sensitive and selective analytical methods. HPLC separation of peptides on a reversed-phase column coupled with UV/Vis detection (220 – 280 nm) has been conventionally used [19]. However, UV/Vis spectroscopy was only able to detect analytes at > μM levels and was susceptible to interference from endogenous contaminants, rendering this method not suitable for quantitative analysis of low concentration analytes in complex biological matrices. In order to augment assay sensitivity and selectivity, chemical derivatization of small amines and peptides with fluorescence probes such as 9-fluorenylmethyl chloroformate (Fmoc) [90], 6-aminoquinolyl-*N*-hydroxysuccinimidyl carbamate (AQC) [91], fluorescamine [92], dansyl chloride (Dns) [93], and naphatalene-2,3-dialdehyde (NDA) [94], etc., coupled with fluorescence spectroscopy was performed. For instance, a fluorescence derivatization reagent NDA has been successfully applied to clarify the *in vivo* oral

absorption of antihypertensive dipeptide VY in human subjects, and tissue distribution and accumulation in SHRs at sub-pmol/mL concentrations [10, 95]. Nonetheless, tedious and complex sample preparation and chromatographic works are still required to separate targeted peptides from endogenous contaminants from biological matrices.

The emergence of electrospray ionization mass spectrometry (ESI-MS) furtherly increased detection sensitivity and selectivity, which enabled rapid detection of peptides in culture media or biofluids at lower molar concentration ranges [19]. For instance, an LC-multiple reaction monitoring (MRM)-MS/MS method has been developed for successive analysis of plasma concentrations of three bioactive dipeptides, VY, MY, and LY, after single oral administration [80]. The LC-MS method was able to selectively detect and quantify them in plasma at pmol/mL levels with high reproducibility (CV < 5%). Even so, a lower limit-of-detection (LOD) is still desirable for systemic elucidation of peptide absorption in a small volume of blood of living animals.

In ESI interface, charged droplets containing analytes are formed during the electrospray process [96]. According to ion evaporation theory, ions “evaporate” from the droplet surface and enter into the gas phase during solvent evaporation [97]. Thus, it is believed that ions (analytes) residing on the droplet surface ionize more readily than ions in the droplet

interior [98]. Hydrophobicity dictates the rate at which analytes migrate to droplet surface [99]. Therefore, to increase ESI-MS signal intensity, efforts have been made to increase the hydrophobicity of amines and peptides, by means of introducing hydrophobic moiety through chemical derivatization. For example, an amine derivatization reagent 3-aminopyridyl-*N*-hydroxysuccinimidyl carbamate (APDS) has been developed and commercialized for rapid ESI-MS detection of common amino acids and other small molecules with amino groups [100]. Also, amino group derivatization by TNBS largely enhanced the ESI detection sensitivity of dipeptides [81] and advanced glycan end-products (AGEs) [82]. However, in contrast to the reported application to small amines and dipeptides, the benefit of chemical derivatization for enhanced ESI detection of longer oligopeptides still needs to be studied.

Therefore, in **Chapter II**, ESI detection characteristics of synthetic oligopeptides with chemical derivatizations were investigated. Model di- to penta-oligopeptides were synthesized on the basis of glycine (Gly, G) and sarcosine (*N*-methylated G; Sar, S) due to their simple chemical structures. Four reported amine derivatization reagents, namely, APDS [100], TNBS [24, 81], NDA [94], and *N*-succinimidyl 7-methoxycoumarin-3-carboxylate (Cou) [101] were used in this study (Figure 2-1).

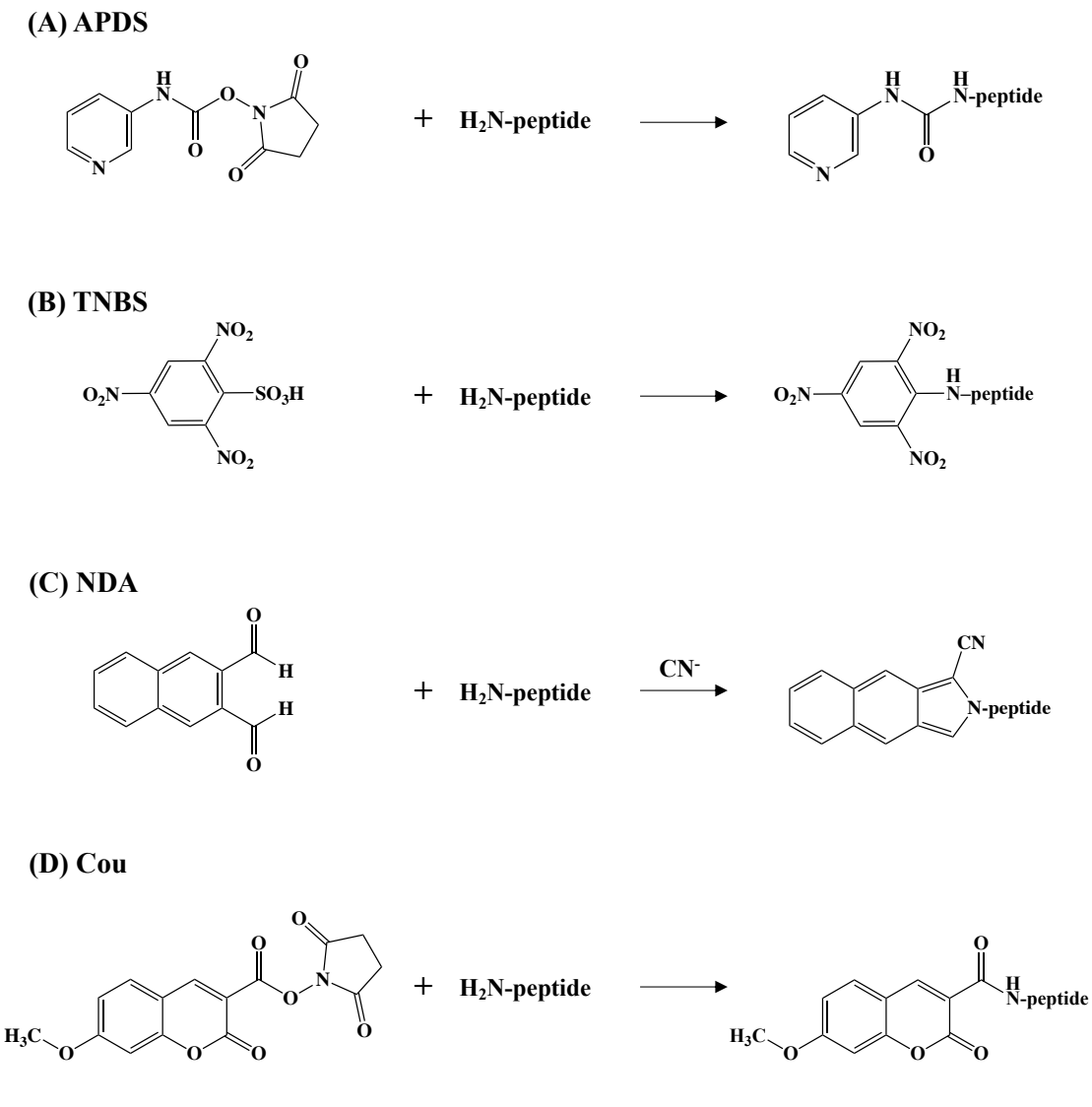

Figure 2-1. Reaction schemes of peptide derivatization reagents used in this study.

2. Materials and methods

2.1. Materials

GG, GGG, and TNBS were purchased from Nacalai Tesque, Inc. (Kyoto, Japan). GS, Cou, and NDA were purchased from Sigma-Aldrich Co. LLC (St. Louis, MO, USA). GSS was purchased from Bachem AG (Bubendorf, Switzerland). GSSS and GSSSS were purchased from Biomatik Corp. (Cambridge, ON, Canada). APDS (APDSTAG®) was purchased from Wako Pure Chemical Industries, Ltd. (Osaka, Japan). GGGG and GGGGG were synthesized manually by a solid phase peptide synthesis using Fmoc-Gly-OH and Fmoc-Gly-Wang resin (100 – 200 mesh) from Kokusan Chemical Co., Ltd. (Tokyo, Japan), respectively. LC-MS grade water, acetonitrile (ACN), and formic acid (FA) were purchased from Merck (Darmstadt, Germany). LC-MS grade methanol (MeOH) was purchased from Kanto Chemical Co., Inc. (Tokyo, Japan). All other chemicals were of analytical reagent grade and were used without further purification.

2.2. Chemical derivatizations of oligopeptides

Chemical derivatizations of oligopeptides were conducted according to previous reports. TNBS derivatization of the oligopeptides was

conducted by adding 50 μL of 150 mmol/L TNBS dissolved in 100 mmol/L borate buffer (pH 8.0) to 50 μL of a standard peptide solution. The mixture was incubated at 30 °C for 30 min. Then 100 μL of 0.2% FA was added to quench the reaction [81]. APDS derivatization was conducted by adding 5 μL of 20 mg/mL APDS dissolved in ACN to 195 μL of a standard peptide solution dissolved in 100 mmol/L borate buffer (pH 8.0). The mixture was incubated at 60 °C for 30 min for reaction [100]. Cou derivatization was conducted by adding 10 μL of 30 μmol/L Cou and 10 μL of 1 mol/L tetraethylammonium bromide to 20 μL of a standard peptide solution. The mixture was incubated at 30 °C for 30 min for reaction [101]. NDA derivatization was conducted by adding 40 μL of 0.1 mmol/L NDA and 10 μL of 1 mmol/L sodium cyanide both dissolved in methanol, to 50 μL of a standard peptide solution dissolved in 100 mmol/L borate buffer (pH 8.0). The mixture was incubated at 30 °C for 50 min for reaction [94]. Peptides were derivatized accordingly to obtain chemically modified oligopeptides at a final concentration of 0.5 μmol/L for LC-ESI-TOF/MS analysis.

2.3. LC-TOF/MS analysis

Targeted intact and derivatized oligopeptides were detected using LC-ESI-TOF/MS. LC separation was performed using an Agilent 1200 series system (Agilent Technologies, Inc., Waldbronn, Germany) on a

Cosmosil 5C_{18}-MS-II column (I.D. 2.0 × 150 mm; Nacalai Tesque, Inc.) at 40 ºC under a linear gradient elution of MeOH containing 0.1% FA (0 – 100% over 20 min) at a flow rate of 0.2 mL/min. An injection volume of 20 µL was used. ESI-TOF/MS analysis was performed using a micrOTOF II (Bruker Daltonik GmbH, Bremen, Germany) in positive ion mode. The ESI conditions were as follows: drying gas (N_2), 8.0 L/min; drying temperature, 200 °C; nebulizing gas (N_2), 1.6 bar; capillary voltage, 3800 V; mass range, *m/z* 100 – 1,000. All data acquisition and analysis were controlled by Bruker Data Analysis 3.2 software. A calibration solution of 10 mmol/L sodium formate in 50% ACN was injected at the beginning of each run, and all spectra were calibrated prior to data analysis. The LC-TOF/MS analyses were repeated 3 times for each of the 8 oligopeptides GG, GGG, GGGG, GGGGG, GS, GSS, GSSS, and GSSSS, and their corresponding APDS, TNBS, Cou, and NDA derivatized peptides.

2.4. Chemical properties of targeted intact and derivatized oligopeptides

The chemical properties, namely, the log *P* and Connolly molecular area (CMA), of targeted intact and derivatized oligopeptides were calculated using a Chem3D Pro. ver. 19.1.0.8 software (PerkinElmer, Inc., Waltham, MA, USA), and are shown in Table 2-1.

Table 2-1. The *m/z*, log *P*, and CMA values of targeted intact and derivatized oligopeptides.

	Residue	*m/z*	CMA (Å^2)	Log *P*
GG	2	133.0608	113.9	-2.015
APDS-GG	2	253.0931	201.7	-1.788
Cou-GG	2	335.0874	254.1	-0.020
NDA-GG	2	308.1030	273.4	2.421
TNP-GG	2	344.0473	238.3	0.347
GGG	3	190.0822	158.1	-2.857
APDS-GGG	3	310.1146	242.2	-2.630
Cou-GGG	3	392.1088	298.3	-0.862
NDA-GGG	3	401.0688	325.4	1.579
TNP-GGG	3	365.1244	282.7	-0.495
GGGG	4	247.1037	235.9	-3.699
APDS-GGGG	4	367.1361	328.9	-3.472
Cou-GGGG	4	449.1303	386.7	-1.704
NDA-GGGG	4	458.0902	377.2	0.737
TNP-GGGG	4	422.1459	352.3	-1.337
GGGGG	5	304.1252	285.8	-4.541
APDS-GGGGG	5	424.1575	378.7	-4.314
Cou-GGGGG	5	506.1518	436.6	-2.546
NDA-GGGGG	5	515.1117	427.1	-0.105
TNP-GGGGG	5	479.1674	402.2	-2.179
GS	2	147.0764	127.0	-1.875
APDS-GS	2	267.1088	209.5	-1.648
Cou-GS	2	349.1030	261.9	0.120
NDA-GS	2	358.0630	290.9	2.561
TNP-GS	2	322.1186	248.1	0.488
GSS	3	218.1135	181.6	-2.577
APDS-GSS	3	338.1459	258.6	-2.350
Cou-GSS	3	420.1401	314.8	-0.582
NDA-GSS	3	429.1001	353.4	1.859
TNP-GSS	3	393.1557	302.6	-0.214
GSSS	4	289.1506	236.4	-3.279
APDS-GSSS	4	409.1830	311.6	-3.052
Cou-GSSS	4	491.1773	367.8	-1.284
NDA-GSSS	4	500.1372	416.9	1.158
TNP-GSSS	4	464.1928	357.5	-0.916
GSSSS	5	360.1878	291.4	-3.981
APDS-GSSSS	5	480.2201	428.3	-3.753
Cou-GSSSS	5	562.2144	484.8	-1.986
NDA-GSSSS	5	571.1743	478.3	0.456
TNP-GSSSS	5	535.2300	447.5	-1.618

CMA: Connolly molecular area

3. Results and discussion

3.1 Detection of targeted intact and derivatized oligopeptides by LC-ESI-TOF/MS

The eight oligopeptides, namely, GG, GGG, GGGG, GGGGG, GS, GSS, GSSS, and GSSSS, were reacted with a variety of chemical derivatization reagents, according to their individual reaction conditions to obtain TNBS-, APDS-, Cou-, and NDA-derivatized oligopeptides (Figure 2-1). Targeted intact and derivatized oligopeptides were analyzed by LC-ESI-TOF/MS. All 40 oligopeptides were detected by the current LC and MS conditions. Typical extracted ion chromatograms (EICs) are shown in Figure 2-2. For each oligopeptide, MS signal intensities were enhanced by derivatization compared to non-derivatized peptide standards, up to ~7 folds depending on the peptides. For di- and tripeptides, hydrophobic tags such as NDA and Cou caused greater signal enhancement. In contrast, for longer peptides such as GSSS and GSSSS, less hydrophobic APDS-tagged peptides showed higher intensities relatively. Exceptions are GGGG and GGGGG (Figure 2-2C and 2D), where the benefit of chemical derivatizations was marginal compared to other peptides. As it is widely believed that more hydrophobic compounds ionize more readily in an ESI droplet [99, 102], the present data suggested that induced hydrophobicity gain through chemical derivatization might not universally lead to

enhanced LC-ESI-MS signal intensity. Particularly, GGGG and GGGGG responded to chemical derivatization very differently from GSSS and GSSSS, despite the fact that these peptides only differ by several methyl groups (Figure 2-2C, 2D, 2G, and 2H). Liigand et al. [103] reported that Gly-βAla-βAla bearing two extra methylene groups showed 4.5-times higher ionization efficiency than GGG. In accordance with their findings, GSSS and GSSSS with extra methyl groups also showed ~ 2-times higher MS signal sensitivity than GGGG and GGGGG. Correspondingly, it could be speculated that even simple side chain structures such as methyl groups could potentially affect the ESI-MS detection and the response to chemical derivatization of oligopeptides.

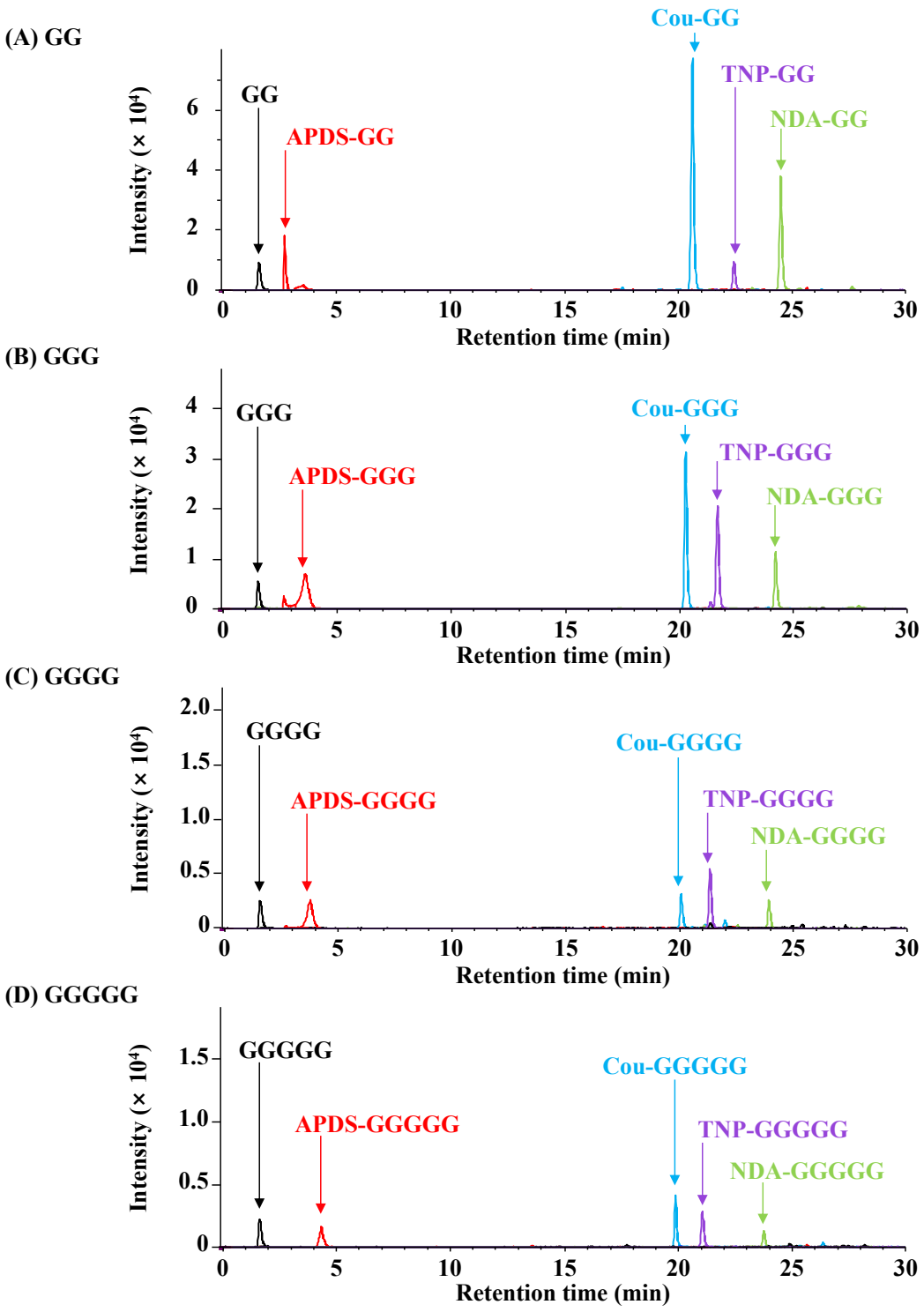

Figure 2-2. Typical LC-ESI-TOF/MS EICs of (A) GG, (B) GGG, (C) GGGG, and (D) GGGGG, and corresponding TNBS-, APDS-, Cou-, and NDA-derivatized oligopeptides, respectively. Continued on the next page.

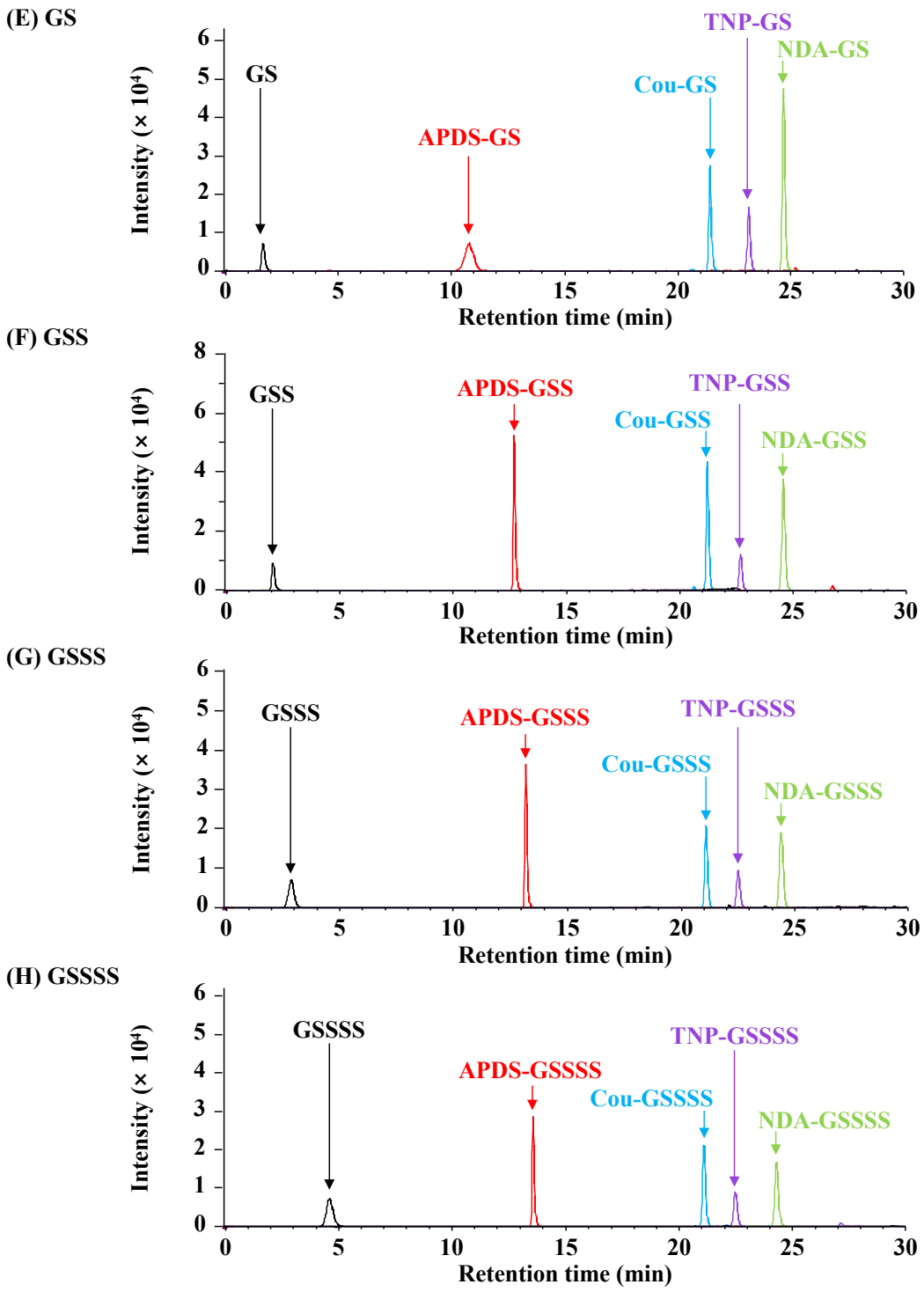

Figure 2-2 (*continued*). Typical LC-ESI-TOF/MS EICs of (E) GS, (F) GSS, (G) GSSS, and (H) GSSSS, and corresponding TNBS-, APDS-, Cou-, and NDA-derivatized oligopeptides, respectively.

MS signal intensity of the derivatized oligopeptides showed a decreasing trend in relation to peptide chain length (Figure 2-3). On the whole, chemically modified di-/tripeptides were detected with higher MS signal intensities compared to longer oligopeptides. For instance, for GG, Cou derivatization led to a maximum of 7-fold stronger signal intensity than non-derivatized GG standard. In contrast, for tetra- and pentapeptides, a maximum of 5-fold increase in MS signal intensity was observed, while in some cases, the MS signal even decreased after derivatization, e.g., NDA derivatized GGGG and GGGGG showed lower MS signal intensities than those of non-derivatized GGGG and GGGGG standards. Overall, the MS signal intensities diminished with an additional Gly or Sar into peptide sequence, suggesting that the MS signal enhancing effect of chemical derivatization might be negligible for longer peptides.

Many studies have been conducted to compare the performance of different derivatization reagents on small amines and peptides [104–106]. However, the current study is the first to investigate the relationship between peptide chain length and performance of derivatization reagents. Using synthetic di- to pentapeptides consisting of Gly and/or Sar and four reported derivatization reagents TNBS, APDS, Cou, and NDA, the present results suggested that shorter di- and tripeptides respond better than longer tetra- and pentapeptides to chemical derivatization as indicated by greater

fold-increase in MS signal intensity on the whole. Mirzaei and Regnier [106] investigated the derivatization of a variety of synthetic peptides with quaternary ammonium salts and concluded that peptides of smaller sizes (less than 500 Da) experienced greater increase in ionization efficiency after derivatization, while for longer peptides such as DRVYIHPFHL, CDPGYIGSR, SYSMEHFRWG, and AFPLEF, derivatization either resulted in slightly decreased ionization efficiency or had little effect. These results are in accordance with the findings in the current study that it is less advantageous for longer oligopeptides to enhance ESI-MS detection via chemical derivatizations.

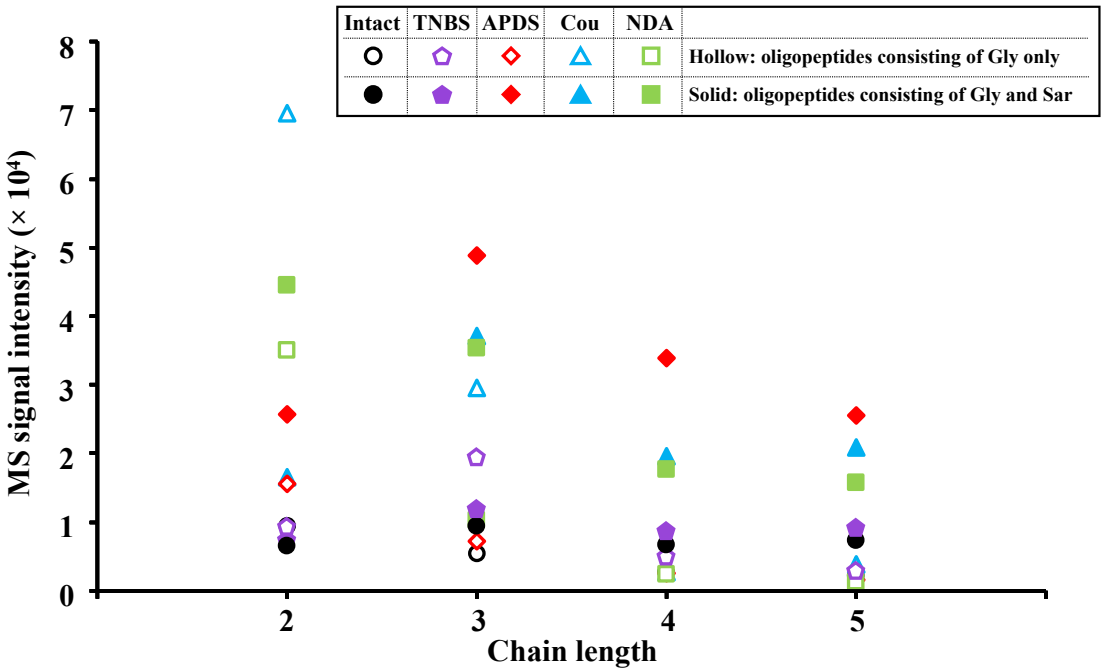

Figure 2-3. Relationship between chain length and MS signal intensity of intact and derivatized oligopeptides. Oligopeptides targeted in this study were GG, GGG, GGGG, GGGGG, GS, GSS, GSSS, and GSSSS.

3.2 Relationship between hydrophobicity and MS signal intensity of oligopeptides

Hydrophobicity has been considered to be related to ionization efficiency in ESI source [99, 102]. In this study, log *P* values were calculated and used to illustrate the hydrophobicity of each oligopeptide. As shown in Table 2-1, log *P* was increased for whichever peptide after chemical derivatization compared to non-derivatized peptide standard. NDA derivatization induced the greatest increase in log *P*, followed by TNBS, Cou, and APDS. As shown in Figure 2-4A, overall, a moderate correlation was observed between MS signal intensity and log *P*. However, for individual peptide, increased hydrophobicity did not necessarily lead to enhanced MS signal intensity (Figure 2-4B). For example, as a peptide could gain the second highest hydrophobicity through TNBS derivatization, the resulting trinitrophenyl (TNP)-tagged peptides showed lower MS signal intensities compared to corresponding peptides modified by other less hydrophobic tags such as Cou and APDS. The three polar, electron-withdrawing nitro groups could render the ionization of TNP-tagged peptides less efficient despite the hydrophobicity gain [107]. In the meantime, for longer oligopeptides GSSS and GSSSS, APDS induced the highest intensity increase despite that it is the least hydrophobic derivatization reagent among the four (Table 2-1). Theoretically, increase

in hydrophobicity would result in increased ionization efficiency [98, 99]. However, as indicated by the results above, it is apparent that hydrophobicity (log *P*) alone is not sufficient to account for the diverse behavior of the 8 tested oligopeptides in response to chemical derivatizations. Hermans et al. examined the effect of acylation on the ESI detection of 14 amino acids using acylation reagents of different sizes, namely, acetic (C2), propionic (C3), butyric (C4), hexanoic (C6) acid anhydride, and polyethylene glycol (PEG) containing five ethylene glycol units. They reported that even for small non-derivatized and corresponding acylated amino acids, while correlations still present for individual amino acids, there is considerable scattering in the correlation between log *P* and ESI response on the whole [107]. Instead, significant correlation between ESI response and calculated molecular volume was observed [107]. In the current study, similarly, weak trends between ESI-MS signal intensity and log *P* could still be observed for di- and tripeptides GG, GS, GGG, and GSS, but not for longer tetra- and pentapeptides. These results suggested that the molecular properties other than hydrophobicity affects the ESI detection more for longer oligopeptides.

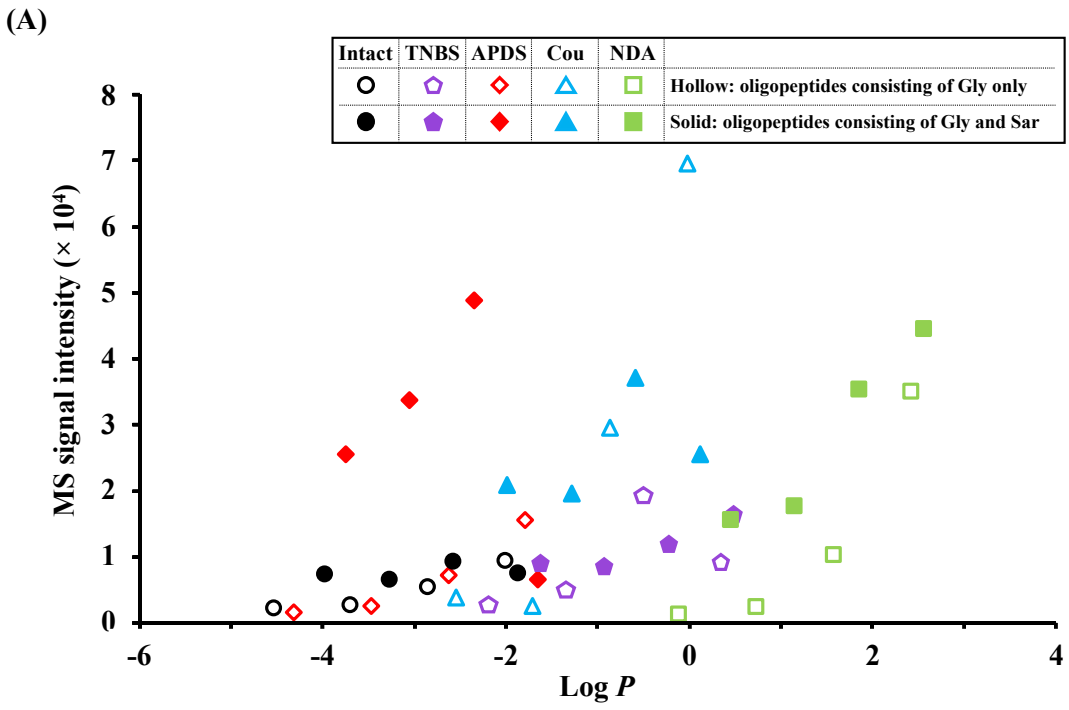

Figure 2-4. (A) Relationship between log *P* and MS signal intensity of targeted intact and derivatized oligopeptides on the whole. Continued on the next page.

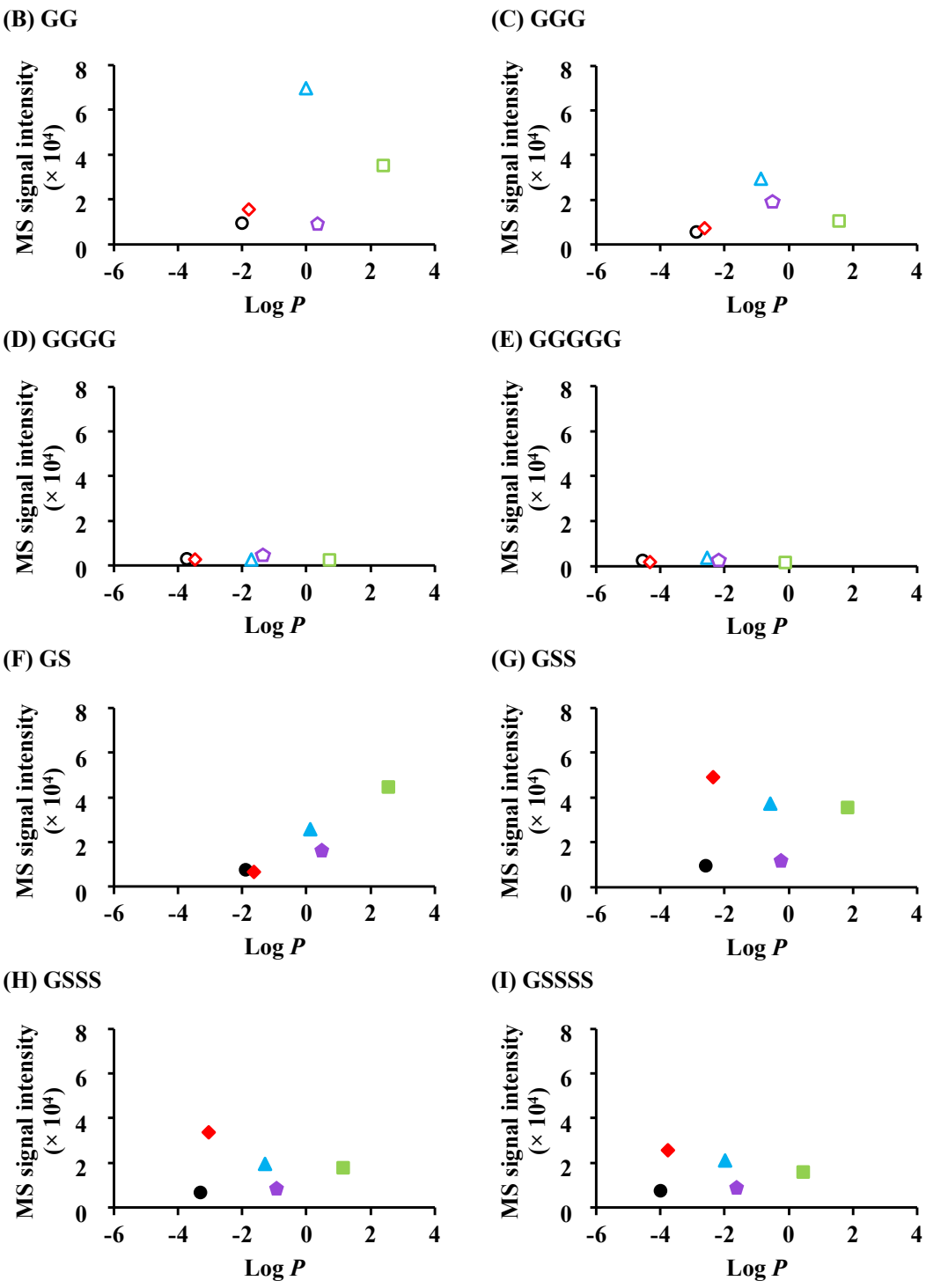

Figure 2-4 (*continued*). Relationship between log *P* and MS signal intensity of targeted intact and derivatized oligopeptides (B) GG, (C) GGG, (D) GGGG, (E) GGGGG, (F) GS, (G) GSS, (H) GSSS, and (I) GSSSS individually.

3.3 Relationship between molecular surface area and MS signal intensity of oligopeptides

Lower MS intensities were observed for longer oligopeptides compared to di-/tripeptides (Figure 2-2), suggesting that the size of a peptide might be related to its MS signal intensity. Therefore, the CMA values of the oligopeptides were calculated to illustrate the respective molecular surface area [108]. As shown in Figure 2-5, the relationship between MS signal intensity and the CMA of the oligopeptides showed a bell-shaped trend, and the highest MS signal intensity was observed between 250 – 300 $Å^2$. Similarly, a linear correlation was reported between MS response and molecular surface area for a series of G-X-G tripeptides smaller than 250 $Å^2$, where X stands for one of the twelve tested amino acids [109]. Moreover, in a study by Randall et al., who investigated the relationship between nonpolar surface area and LC-MS response, it was demonstrated that addition of hydrophobic tags was only effective for molecules of restricted sizes, while further increase in peptide size and hydrophobicity rather diminished MS signal [110]. Although there are still other aspects that have to be considered, it is indicated that the size of a peptide might be related to its ESI-MS signal intensity. As a result, addition of bulky hydrophobic tags to enhance ESI-MS detection might be less advantageous for longer peptides rather than for di-/tripeptides.

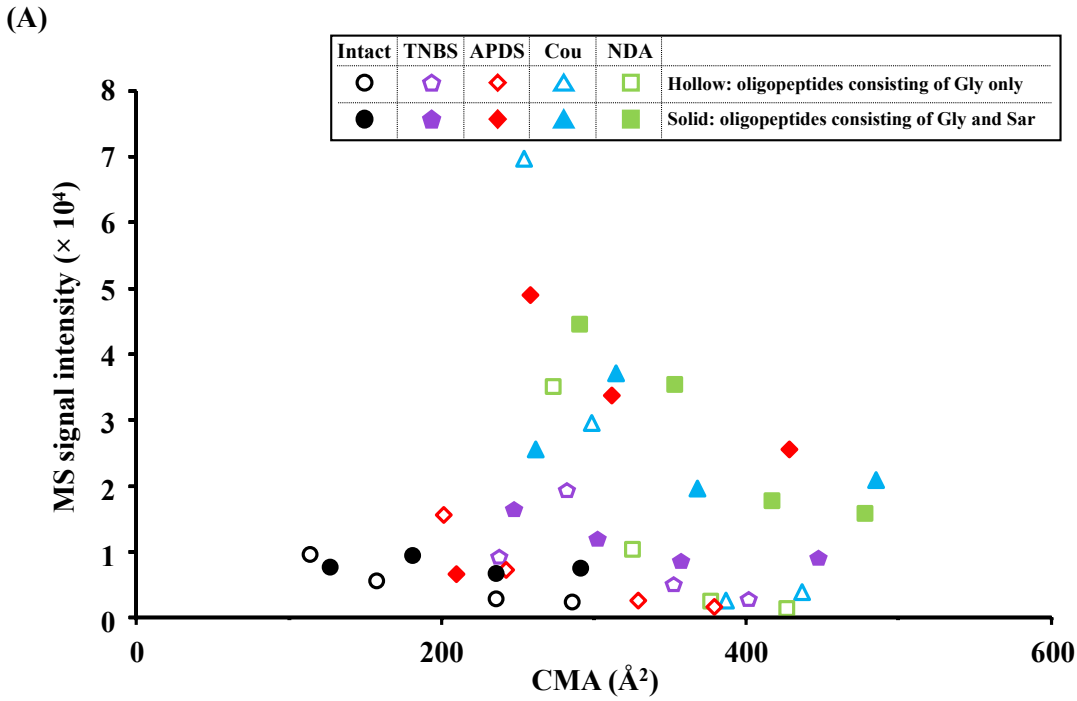

Figure 2-5. (A) Relationship between CMA and MS signal intensity of targeted intact and derivatized oligopeptides on the whole. Continued on the next page.

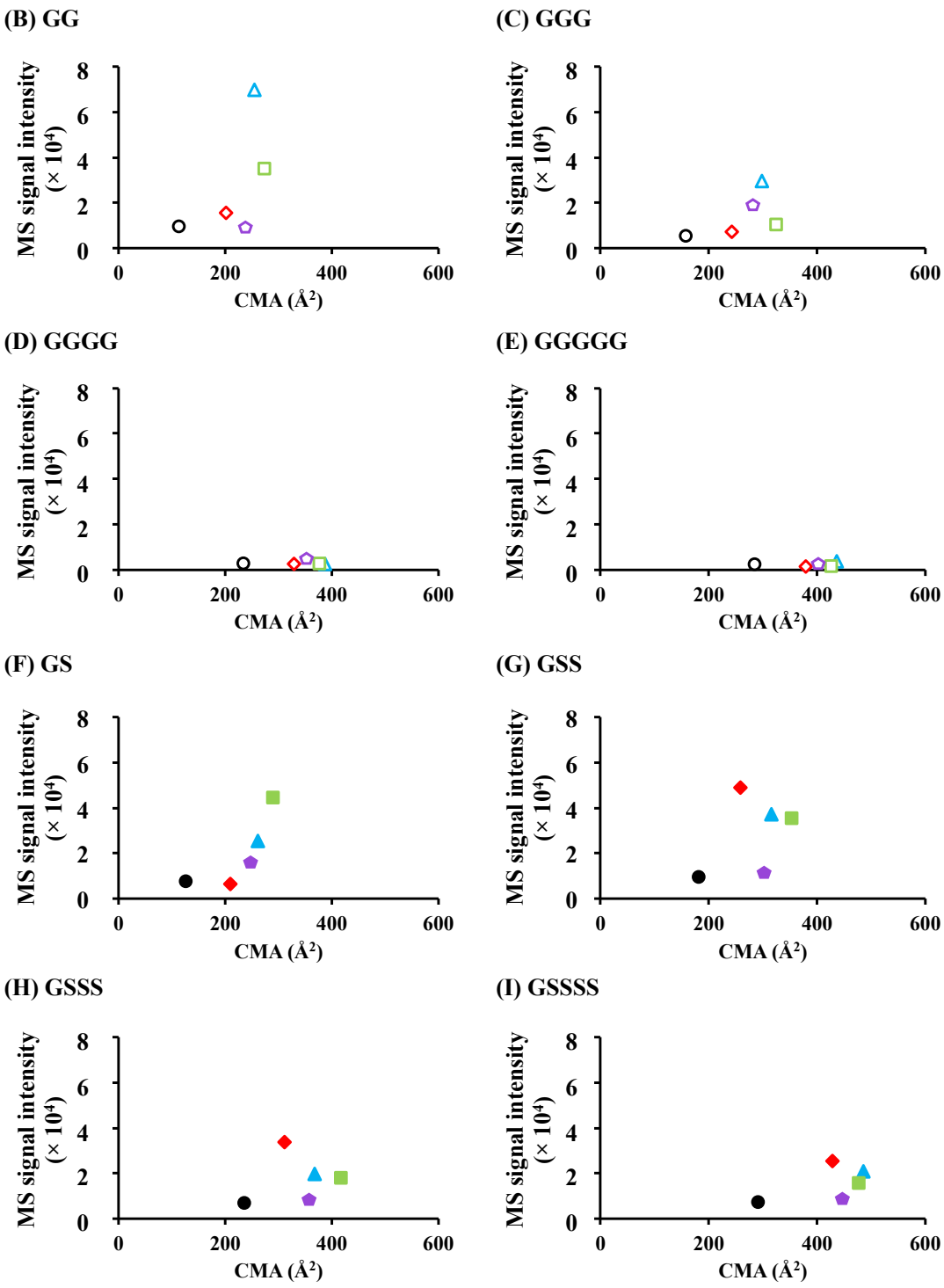

Figure 2-5 (*continued*). Relationship between CMA and MS signal intensity of targeted intact and derivatized oligopeptides (B) GG, (C) GGG, (D) GGGG, E (GGGGG), F (GS), G (GSS), H (GSSS), and I (GSSSS) individually.

Chemical derivatization has been conventionally used for enhancing detection of small amines and peptides [111]. However, in the current study, it is demonstrated that rather than log *P*, the size of a peptide is related to its ESI-MS signal intensity, and that the benefit of chemical derivatization peptides might be negligible for longer, bigger-sized peptides. It is observed that basic amino acids such as Lys, Arg, and His possess higher ionization efficiencies since these amino acids present in positively charged states in solution [112]. Based on this notion, there are attempts to introduce a moiety bearing permanent positive charges to enhance MS detection [113]. However, such applications are mainly used for the detection of inherently poorly ionizable molecular species, such as fatty acids in positive ion mode [114, 115], and for omics studies targeting small molecules [116]. Actually, Mirzaei and Regnier [106] evaluated the performance of two quaternary ammonium salts bearing positive charges on peptides and concluded that the methods worked predominantly for small (< 500 Da) and poorly ionized peptides. Nonetheless, chemical derivatization is still a valuable technique to enhance chromatographic separation [117], to facilitate quantitative isobaric proteome analysis [118], and to separate and identify optical isomers [119], etc.

In the current study, Gly with a single hydrogen as its side chain was selected to be the peptide skeleton. It should be noted that Gly is rather

hydrophilic, and its ionization efficiency is rather poor among 20 common amino acids [103]. However, as demonstrated in the current study, even for hydrophilic oligopeptides consisting of Gly and/or Sar, introduction of hydrophobic moieties did not perform as well compared to smaller di-/tripeptides and was almost ineffective for GGGG and GGGGG. Rather, the ESI-MS detection was dependent on peptide size. The current study ignored the complicated side chain structures. Existence of amino acids other than Gly, especially hydrophobic or basic amino acids Leu, Phe, His, Arg, and Lys could potentially affect peptide ionization efficiency [112]. However, it might be hard to specifically increase the detection sensitivity of long oligopeptides [106]. Even so, there are still other possible approaches, for example, through boosting the efficiency of desolvation, by adding proper post-column solvent additives [120] or minimizing flow rate [121, 122].

4. Summary

Food derived small peptides are believed to potentially play a role in health promotion. Upon oral intake, absorption of such peptides in their intact peptide forms is essential for their functions. The elucidation of the bioavailability of bioactive peptides relies on robust analytical methods such as LC separation of peptides coupled with MS detection. Chemical derivatization of small peptides has been demonstrated to be able to increase MS detection sensitivity and thus enhance peptide detection at lower molar concentration ranges. However, the advantages of chemical derivatization on longer oligopeptides remain unclear. In this Chapter, ESI-MS detection of synthetic di- to pentapeptides GG, GGG, GGGG, GGGGG, GS, GSS, GSSS, and GSSSS by four amine derivatization methods, TNBS, APDS, Cou, and NDA was characterized. All 40 non-derivatized and chemically modified oligopeptides were successfully detected by the current LC-MS settings. Overall, chemically modified di-/tripeptides were detected with higher MS signal intensities than tetra-/pentapeptides, suggesting that chemical derivatization might be more advantageous for small di-/tripeptides than longer oligopeptides as a means to enhance MS detection. For individual peptides, increase in hydrophobicity did not necessarily lead to intensity enhancement. Meanwhile, oligopeptides with CMA values between 250 – 300 $Å^2$ showed

the highest MS intensity, indicating that molecular surface area may be a determining factor of ESI-MS signal intensity of oligopeptides.

Chapter III

Intestinal absorption of Cblin pentapeptides in Caco-2 cells and Sprague-Dawley rats

1. Introduction

Cbl-b inhibitory (or Cblin) oligopeptides are composed of two pentapeptides DGpYMP and DGYMP (Figure 3-1) corresponding to the 606 to 610 residues of insulin receptor substrate-1 (IRS-1), a key intracellular molecule of insulin-like growth factor-1 (IGF-1) signaling pathway that is involved in muscle growth and hypertrophy [83, 123]. Ubiquitin ligase Cbl-b is a key molecule in the IGF-1 mediated muscle synthesis and proteolysis. When experiencing unloading stresses, such as bedridden due to sickness or old age, and microgravity associated with space flight, etc., it was demonstrated that the expression of ubiquitin ligase Cbl-b was elevated [88]. Cbl-b induces ubiquitination and degradation of IRS-1, which eventually leads to muscle loss [83]. Cblin peptides DGpYMP and DGYMP have been demonstrated to be able to interfere

with the ubiquitination of IRS-1 by inhibiting ubiquitin ligase Cbl-b, thus ameliorate IGF-1 resistance induced by unloading stress and block the ubiquitin-dependent proteolysis of skeletal muscles (Figure 3-1) [83, 124]. Intramuscular injection of Cblin peptides to denervated mice significantly prevented the ubiquitination of IRS-1 and muscle loss [83]. However, repetitive invasive procedures such as intramuscular injection could be stressful. Meanwhile, oral intake of Cblin oligopeptides has been considered as an alternative approach to prevent disuse muscle atrophy caused by unloading stress.

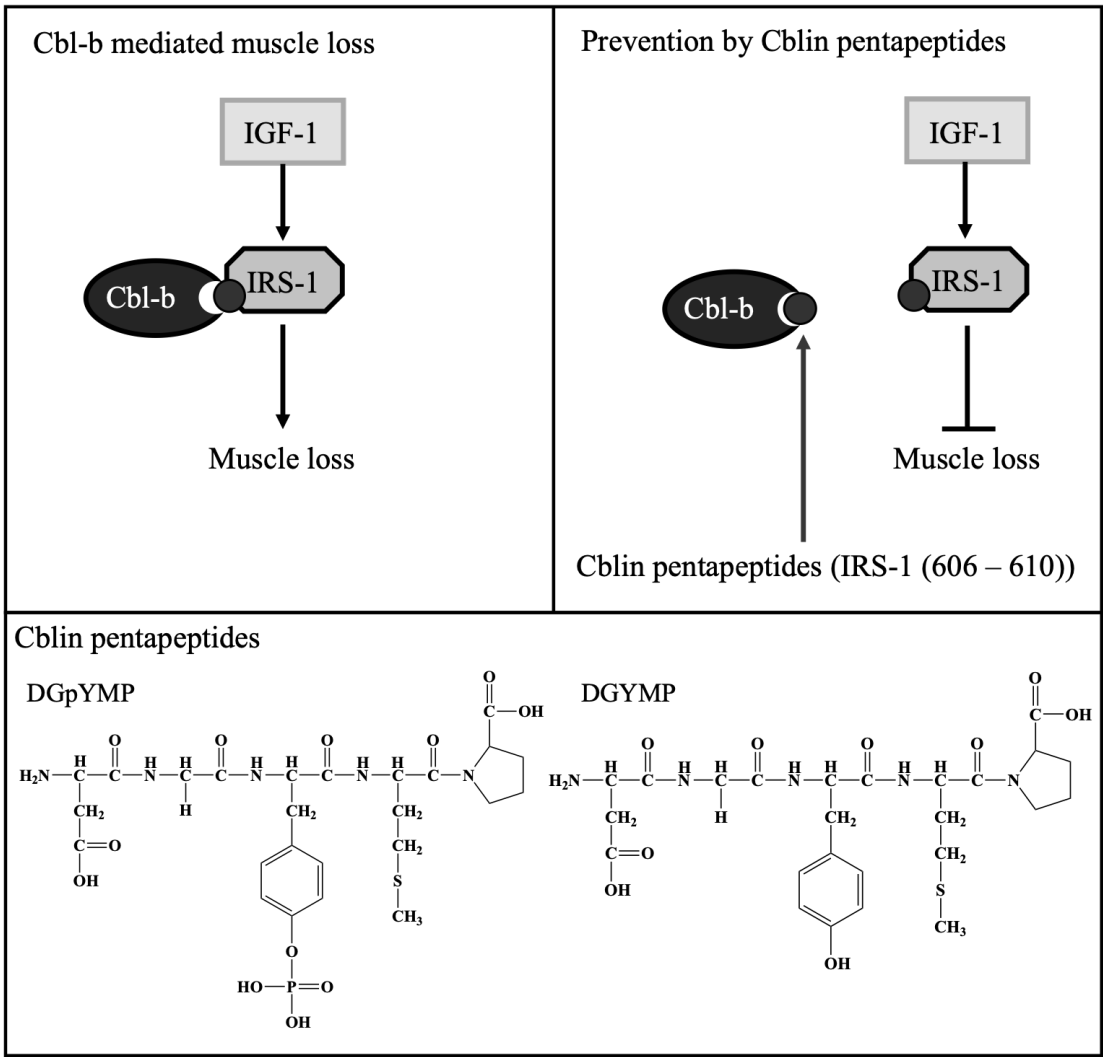

Figure 3-1. The structures of Cblin pentapeptides and their mechanism to prevent disuse muscle atrophy by inhibiting Cbl-b mediated proteolysis.

Upon oral intake, Cblin oligopeptides need to be absorbed into blood circulation across the small intestine and reach muscle cells in their intact peptide forms to elicit their bioactivities. The intestinal PepT1 has been extensively studied regarding its role on the absorption of di-/tripeptides [9, 19, 24]. In the meantime, for longer peptides, although currently no transporter is known, a series of *in vitro* Caco-2 cell studies indicated that oligopeptides still could be absorbed via paracellular or transcellular routes [19]. However, it should be noted that Caco-2 cell studies may not necessarily reflect the *in vivo* absorption [24]. In contrast to the Caco-2 cell studies, few studies have been conducted and large remains unknown regarding the *in vivo* absorption of longer oligopeptides in animal models.

Complex sample matrices and relatively low concentrations of peptides are considered as the bottlenecks for the elucidation of peptide absorption *in vivo*. However, with the implementation of LC-MS, higher sensitivity and selectivity were achieved compared to conventional HPLC-UV/Vis assays. A series of di- to penta- model peptides GS, GSS, GSSS, and GSSSS were designed and synthesized [117]. With the aid of chemical derivatization technique, LC-ESI-TOF/MS was successfully applied to study the intestinal absorption behavior of these peptides in spontaneously hypertensive rats (SHRs). It was shown that in addition to GS and GSS, longer oligopeptides GSSS and GSSSS were also detected in rat blood

circulation, indicating that oligopeptides with more than three amino acid residues could also be absorbed in their intact peptide forms *in vivo* [125]. Therefore, in Chapter III, the high sensitivity and selectivity of LC-ESI-TOF/MS were exploited to investigate the intestinal absorption of disuse muscle atrophy preventive Cblin pentapeptides DGpYMP and DGYMP, using Caco-2 cells *in vitro* and SD rats *in vivo*.

2. Materials and methods

2.1. Materials

Dulbecco's modified Eagle's medium (DMEM) and fetal bovine serum (FBS) were purchased from Thermo Fisher Scientific Inc. (Gibco^{TM}; Waltham, MA, USA). Nonessential amino acid mixture was purchased from MP Biomedicals, LLC (Irvine, CA, USA). Penicillin was purchased from Meiji Seika Pharma Co., Ltd. (Tokyo, Japan). Streptomycin, L-glutamine, and 2-(*N*-morpholino)ethanesulfonic acid (MES) were purchased from Nacalai Tesque, Inc. (Kyoto, Japan). *N*-2-Hydroxyethylpiperazine-*N*'-2-ethanesulfonic acid (HEPES) and cytochalasin D were purchased from Wako Pure Chemical Industries, Ltd. (Osaka, Japan). Gly-Sar was purchased from Sigma-Aldrich Co. LLC (St. Louis, MO, USA). Cblin peptides DGYMP, DGpYMP, and [$^{13}C_2$,^{15}N] Gly-labeled-DGYMP were purchased from Scrum Inc. (Tokyo, Japan). Hank's balanced salt solution (HBSS) buffer was composed of 137 mmol/L NaCl, 5 mmol/L KCl, 5.5 mmol/L D-glucose, 4 mmol/L $NaHCO_3$, 0.75 mmol/L $NaHPO_4 \cdot 12H_2O$, 0.4 mmol/L KH_2PO_4, 0.8 mmol/L $MgSO_4 \cdot 7H_2O$, 1.26 mmol/L $CaCl_2 \cdot 2H_2O$, all obtained from Nacalai Tesque, Inc., with the addition of 10 mmol/L MES or 10 mmol/L HEPES to adjust the pH to 6.0 or 7.4 for apical or basolateral HBSS buffer, respectively. LC-MS grade water, ACN, and FA were purchased from Merck (Darmstadt, Germany).

LC-MS grade MeOH was purchased from Kanto Chemical Co., Inc. (Tokyo, Japan). All other chemicals were of analytical reagent grade and were used without further purification.

2.2. Cell culture

Caco-2 cells from passages 50 – 60 were used in this study. Cells were cultured in DMEM supplemented with 10% FBS, 1% nonessential amino acids, 2 mol/L L-glutamine, 100 U/mL penicillin, 100 μg/L streptomycin, and 1.7 mmol/L insulin in a CO_2 incubator (37 °C, 5% CO_2). The medium was changed once every two days until the cells reached subconfluence. For Caco-2 cell monolayer transport experiments, cells were seeded at a density of 4×10^5 cells/mL to Falcon® cell culture inserts (PET, 1.0 μm pore size; Corning Inc., NY, USA) coated using Collagen Gel Culturing Kit (Nitta Gelatin Inc., Osaka, Japan). The inserts were mounted in 12-well plates. Cells were seeded and cultured for 48 h in DMEM containing 0.1% MITO+ serum extender (Corning Inc.) for cell attachment. Then the medium was replaced with Entero-STIM enterocyte differentiation medium (Corning Inc.) containing 0.1% MITO+ serum extender. The medium was changed every day for 3 days to form Caco-2 cell monolayers. The integrity of the monolayers was evaluated by measuring the transepithelial electrical resistance (TEER) using a Millicell

ERS-2 epithelial voltohmmeter (Merck, Darmstadt, Germany). Monolayers with TEER values of > 300 $\Omega \cdot cm^2$ were used for transport experiment.

2.3. Transport experiment of Cblin pentapeptides across Caco-2 cell monolayers

Caco-2 cell monolayers were cultured in DMEM supplemented with 10% FBS for 24 h before transport experiments. Medium was removed, and monolayers were washed by HBSS buffer twice. Then an aliquot (1.5 mL) of HBSS buffer containing MES (pH 6.0) was added to the apical side and HBSS buffer containing HEPES (pH 7.4) was added to the basolateral side. After equilibrium in a CO_2 incubator (37 °C, 5% CO_2) for 15 min, transport experiments were started by replacing the apical solution with 1.5 mL of 1.0 mmol/L peptide standards dissolved in HBSS (pH 6.0). The plates were incubated in a CO_2 incubator for 60 min and an aliquot (60 μL) was sampled every 15 min. The samples were stored at -30 °C until LC-TOF/MS analysis.

The apparent permeability coefficient (P_{app}, cm/s) was calculated according to the following equation:

$$P_{app} = \frac{dC}{dt} \times \frac{V}{AC_0}$$

where dC/dt is the change in concentration in the basolateral side over time (mM/s), V is the volume of solution in the basolateral compartment (1.5 mL), A is the surface area of the membrane (0.9 cm^2), and C_0 is the initial concentration of the peptides in the apical side (mmol/mL).

For transport route studies, Caco-2 cell monolayers were preincubated with either 10 mmol/mL Gly-Sar as a PepT1 substrate [126], or 0.5 μg/mL cytochalasin D as a tight junction opener [127] for 30 min. Then transport experiments of Cblin pentapeptides were performed as described in the section 2.3, in the presence of Gly-Sar or cytochalasin D.

2.4. Single oral administration experiments

SD rats (SPF/VAF Crj:SD, 7-week-old, male) were purchased from Charles River Laboratories Japan, Inc. (Kanagawa, Japan). The rats were housed for 1 week under controlled temperature of 21 ± 1 ºC, humidity of 55 ± 5%, light scheduled from 8:00 to 20:00, with access to a laboratory diet (MF, Oriental Yeast Co., Ltd., Tokyo, Japan) and water *ad libitum*. The rats were fasted for 16 h before single oral administration experiments. DGYMP at a dose of 100 mg/kg-B.W. dissolved in milli-Q (~1 mL) was given by an oral gavage. Serial blood samples (~300 μL) were collected at 0, 15, 30, 45, and 60 min after administration from the tail vein of each rat

into chilled microtubes containing EDTA (0.2 mg) and protease inhibitors (aprotinin, 0.1 mg; chymostatin, 0.1 mg). Plasma samples were obtained immediately by centrifugation at 3,500 *g* at 4 ºC for 15 min.

Quantitative analysis of DGYMP in plasma samples was performed using internal standard method. To 100 μL of plasma, 10 μL of [$^{13}C_2$,^{15}N] Gly-labeled DGYMP was added to a final concentration of 50 pmol/mL upon analysis. After adequate mixing, protein was precipitated by adding 2 volumes of ice-cold ACN containing 0.1% FA. The samples were then centrifuged at 14,000 *g* at 4 ºC for 15 min. The supernatant was collected and dried using a vacuum evaporator and stored at -30 °C. Upon analysis, the resultant was reconstituted with 25 μL of 0.1% FA, and 20 μL was injected to the LC-ESI-TOF/MS.

All the animal experiments were performed according to the Guidelines for Animal Experiments in the Faculty of Agriculture in the Graduate Course of Kyushu University and according to the Law (No. 105, 1973) and Notification (No. 6, 1980 of the Prime Minister's Office and No. 71, 2006, of the Ministry of Health, Labor and Welfare) of the Japanese Government. All the experiments were reviewed and approved by the Animal Care and Use Committee of Kyushu University (permit number: A30-015-4).

2.5. LC-TOF/MS analysis

Peptide detection and quantification was performed using LC-ESI-TOF/MS. LC separation was performed using an Agilent 1200 series system (Agilent Technologies, Inc., Waldbronn, Germany) on a Cosmosil 5C_{18}-MS-II column (I.D. 2.0 × 150 mm; Nacalai Tesque, Inc.) at 40 ºC under a linear gradient elution of MeOH containing 0.1% FA (0 – 100% over 20 min) at a flow rate of 0.2 mL/min. An injection volume of 20 μL was used. ESI-TOF/MS analysis was performed using a micrOTOF II (Bruker Daltonik GmbH, Bremen, Germany) in positive ion mode. The ESI conditions were as follows: drying gas (N_2), 8.0 L/min; drying temperature, 200 °C; nebulizing gas (N_2), 1.6 bar; capillary voltage, 3800 V; mass range, *m/z* 100 – 1,000. All data acquisition and analysis were controlled by Bruker Data Analysis 3.2 software. A calibration solution of 10 mmol/L sodium formate in 50% ACN was injected at the beginning of each run, and all spectra were calibrated prior to data analysis. For quantification, extracted ion chromatograms were created for each peptide: DGYMP, *m/z* 582.2228; DGpYMP, *m/z* 662.1625; [$^{13}C_2$,^{15}N] Gly-labeled DGYMP, *m/z* 585.2228. Samples from Caco-2 transport experiments were injected to the LC-MS system without any pretreatment. The amounts of peptides were quantified using absolute standard curve method. The equations were: DGYMP: y = 1500209 x + 279590, 0.1 – 10 nmol/mL, *r*

= 1.000, and DGpYMP: y = 701098 x – 47107, 0.1 – 10 nmol/mL, r = 0.9995, where y is the peak area and x is the peptide concentration (nmol/mL). Plasma samples from SD rat single oral administration experiments were pretreated as stated in the section 2.4. and quantification was performed using internal standard method. The equation was: DGYMP: y = 0.0464x – 0.0245, 10 – 100 pmol/mL, r = 0.9982, where y is the peak area ratio (observed peak area of DGYMP against [$^{13}C_2$,^{15}N] Gly-labeled-DGYMP) and x is the peptide concentration (pmol/mL).

2.6. Statistical analysis

Pharmacokinetic parameters C_{max} and t_{max} were determined from 0 to 60 min after oral administration, according to the results of LC-TOF/MS analysis. The elimination rate constant (k) was determined by linear regression analysis of data points plotted between C_{max} and 60 min. The elimination half-life ($t_{1/2}$) was calculated using the equation $t_{1/2} = 0.693/k$. The area under the plasmatic concentration – time curve ($AUC_{0-60\,min}$) was calculated using the trapezoidal rule. All data are expressed as the mean ± SEM. The statistical significance between two groups was evaluated by unpaired Student's t-test. A p-value < 0.05 was considered significant. All pharmacokinetic calculations and statistical analyses were carried out

using GraphPad Prism 5 software (GraphPad Software Inc., San Diego, CA, USA).

3. Results and discussion

3.1. Caco-2 cell transport of Cblin pentapeptides

The LC-ESI-TOF/MS signal intensity of intact DGYMP was approximately 5×10^4, which was comparable to some of the derivatized oligopeptides of the highest intensities, such as Cou-GG, NDA-GS, and APDS-GSS (Figure 2-2 and Figure 3-2). The MS signal intensity of DGYMP was much higher than non-derivatized GGGGG and GSSSS of the same length, even though there is no basic or hydrophobic amino acids such as His, Arg, Lys, etc., which may facilitate ionization [103]. Chemical derivatization did not furtherly enhance the MS signal intensity of DGYMP (Figure 3-2), which was in accordance with our observation that the effect of chemical derivatization might be negligible for longer oligopeptides. Even more, decreases in MS signal intensities were observed for chemically modified DGYMP compared to non-derivatized DGYMP standard. In agreement with our results, it was reported that derivatization of several oligopeptides of 6 to 10 amino acid residues resulted in decreased ionization efficiency [106]. Therefore, in this study, Cblin pentapeptides DGpYMP and DGYMP were subjected to LC-ESI-TOF/MS analysis directly without chemical derivatization.

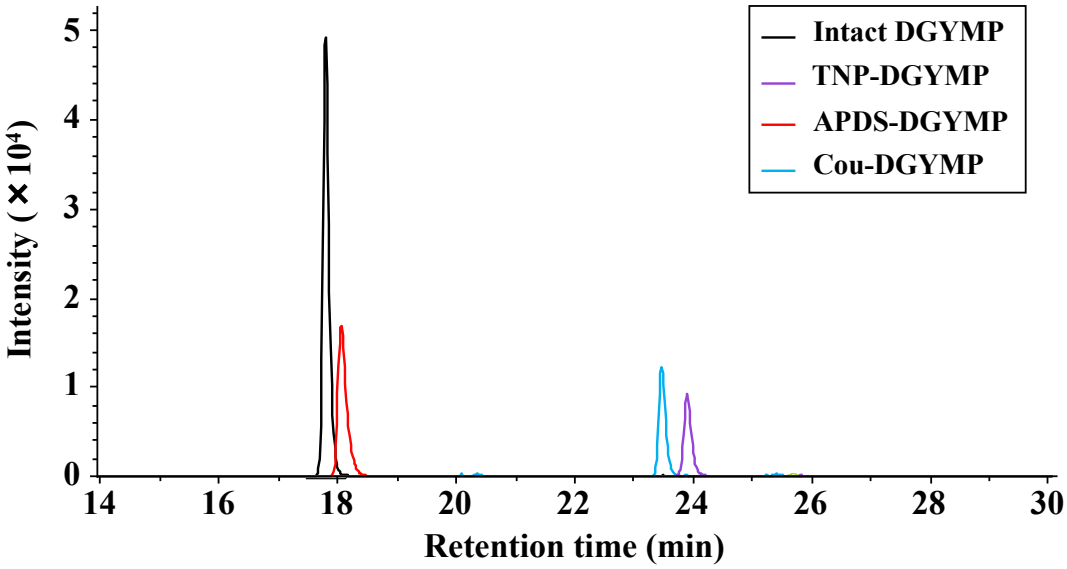

Figure 3-2. Typical LC-ESI-TOF/MS overlaid EICs of DGYMP standard and DGYMP derivatized with APDS, Cou, and TNBS.

Cblin peptides DGpYMP and DGYMP were subjected to Caco-2 cell transport experiments to examine their intestinal permeability. An initial concentration of 1 mmol/L peptide dissolved in HBSS was applied to the apical side and solutions were sampled from basolateral side every 15 min for 60 min. The samples were analyzed by LC-TOF/MS. Figure 3-3 shows the typical LC-TOF/MS stacked extracted ion chromatograms (EIC) of the peptides from 15 to 60 min. Both DGpYMP (*m/z* 662.1625) and DGYMP (*m/z* 582.2228) were detected in the basolateral solution samples, and the concentrations of the peptides increased in a time-dependent manner from 15 to 60 min, showing that Cblin peptides could penetrate Caco-2 cell monolayers in their intact peptide forms.

The apparent permeability coefficient (P_{app}) is used as a parameter to evaluate the transport velocity of peptides across Caco-2 cell monolayers [19]. In previous studies, a series of di- to penta- model oligopeptides for intestinal transport was constructed based on the structure of Gly-Sar [117]. These peptides, which possess high resistance against enzymatic degradation due to their methylated peptide bonds, have been demonstrated to be transportable across Caco-2 cell monolayers [117] and absorbable upon oral administration [125]. As a model pentapeptide for intestinal transport, the P_{app} value for GSSSS was $8.6 \pm 0.6 \times 10^{-7}$ cm/s [117]. In the current study, the P_{app} value was $3.5 \pm 1.2 \times 10^{-7}$ cm/s for DGpYMP and

$7.0 \pm 0.8 \times 10^{-7}$ cm/s for DGYMP. These values are on the same order as the P_{app} of GSSSS, as well as some other pentapeptides such as VLPVP (0.7×10^{-7} cm/s, [49]), QIGLF (9.1×10^{-7} cm/s, [51]), IWHHT (2.2×10^{-7} cm/s, [30]), YFCLT (1.1×10^{-7} cm/s, [54]), etc., that has been reported to be transportable across Caco-2 cell monolayers. Therefore, it is indicated that Cblin pentapeptides DGpYMP and DGYMP could be transported across Caco-2 cell monolayers at appropriate velocities that are comparable to model pentapeptide GSSSS.

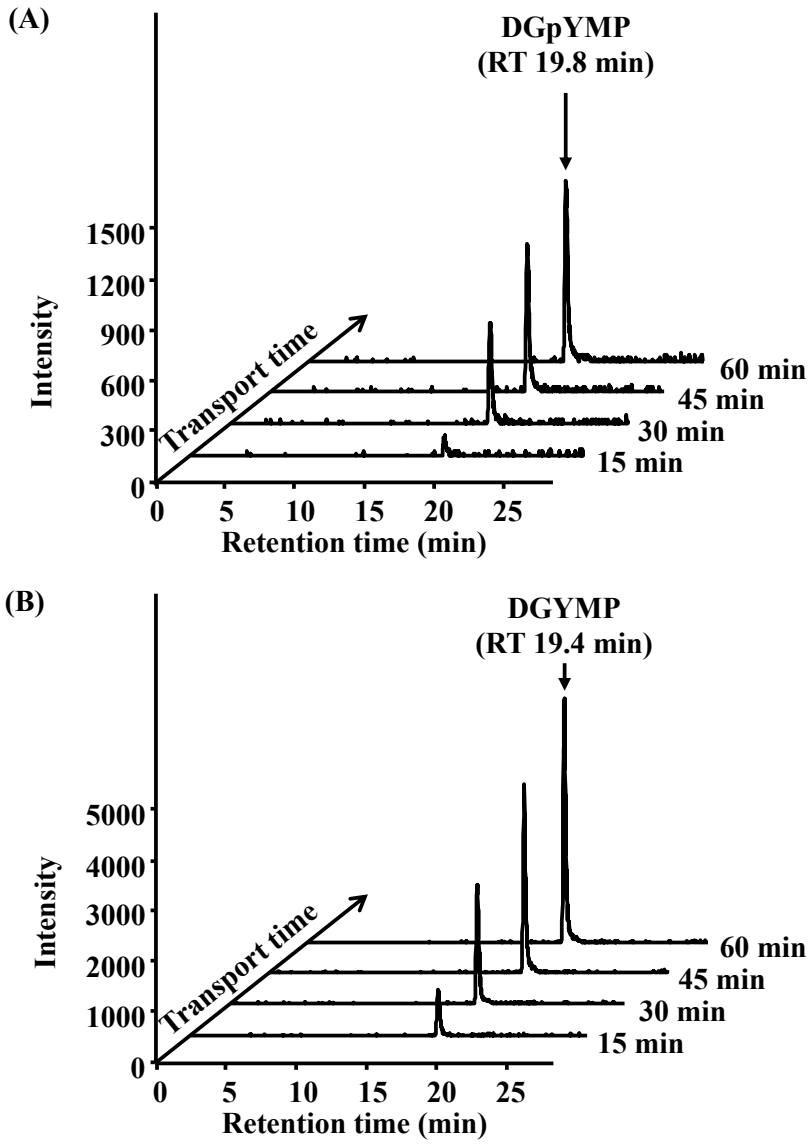

Figure 3-3. Typical LC-ESI-TOF/MS stacked intensity – time EICs for apical to basolateral transport of DGpYMP ($[M + H]^+$ *m/z* 662.1625, (A)) and DGYMP ($[M + H]^+$ *m/z* 582.2228, (B)) across Caco-2 cell monolayers. Transport experiments of 1 mmol/L peptide solutions were performed using Caco-2 cell monolayers for 60 min, respectively. Solutions were sampled from the basolateral side at 15, 30, 45, and 60 min, and were analyzed by LC-TOF/MS.

Peptides might be metabolized by digestive proteases and peptidases into shorter peptide fragments and amino acids in the small intestine [24, 128, 129]. Therefore, a screening of peptide metabolites was conducted by extracting ions of *m/z* values of predicted peptide fragments. As shown in Figure 3-4 (A), DGYMP was found to be a major metabolite in the basolateral solutions after 60 min transport of DGpYMP, indicating that DGpYMP underwent dephosphorylation during the transport process. It is possible that density-enhanced protein phosphatase-1 or intestinal alkaline phosphatase expressed on the surface of Caco-2 cells or secreted into media might be involved this process [16, 130, 131]. Otherwise, no peptide fragments were detected from the basolateral solutions of DGYMP and DGpYMP transport (Figure 3-4B). A pentapeptide IWHHT was found to be cleaved to generate IWH and IW during Caco-2 transport [30]. A pentapeptide GPRGP was found to be cleaved to generate GPR during Caco-2 transport [40]. As such, in Caco-2 cell studies, oligopeptides have been found to be susceptible to enzymatic degradation [23, 45, 50, 65, 68, 75]. Compared to these peptides, Cblin pentapeptides DGpYMP and DGYMP exhibited resistance against proteases and peptidases during Caco-2 cell monolayer transport. There still could be metabolites that cannnot be detected by the current LC-TOF/MS settings. However, the time-dependent transport of the two Cblin oligopeptides (Figure 3-3) suggested that the apical peptide concentrations were maintained to some

extent during the 60 min-transport. The above results suggested that Cblin pentapeptides DGpYMP and DGYMP are resistant to *in vitro* digestion by proteases and peptidases during their transport across Caco-2 cell monolayers to a certain degree.

(A)

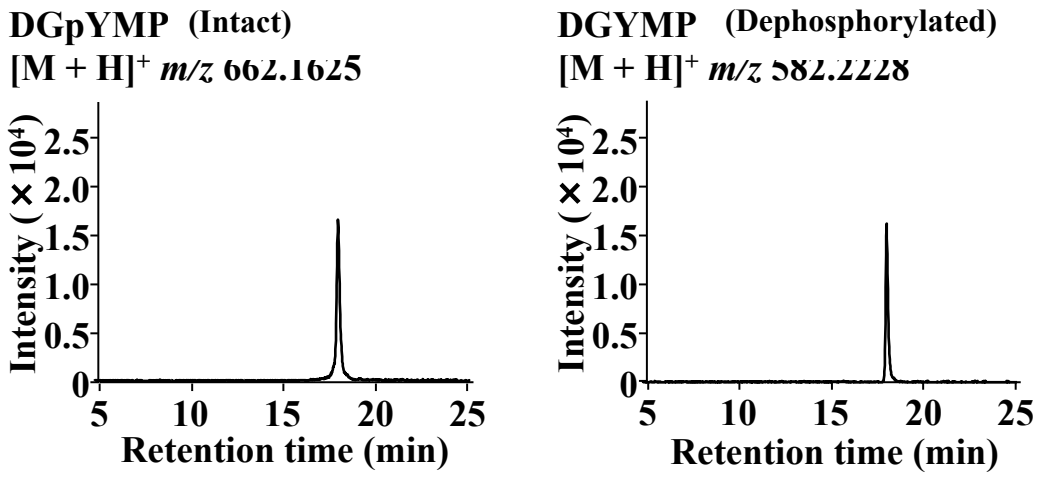

Figure 3-4. (A) Typical LC-ESI-TOF/MS EICs of peptide fragments after 60 min-transport of DGpYMP across Caco-2 cell monolayers. Dephosphorylated DGYMP was detected in basolateral solutions as a dephosphorylated metabolite of DGpYMP.

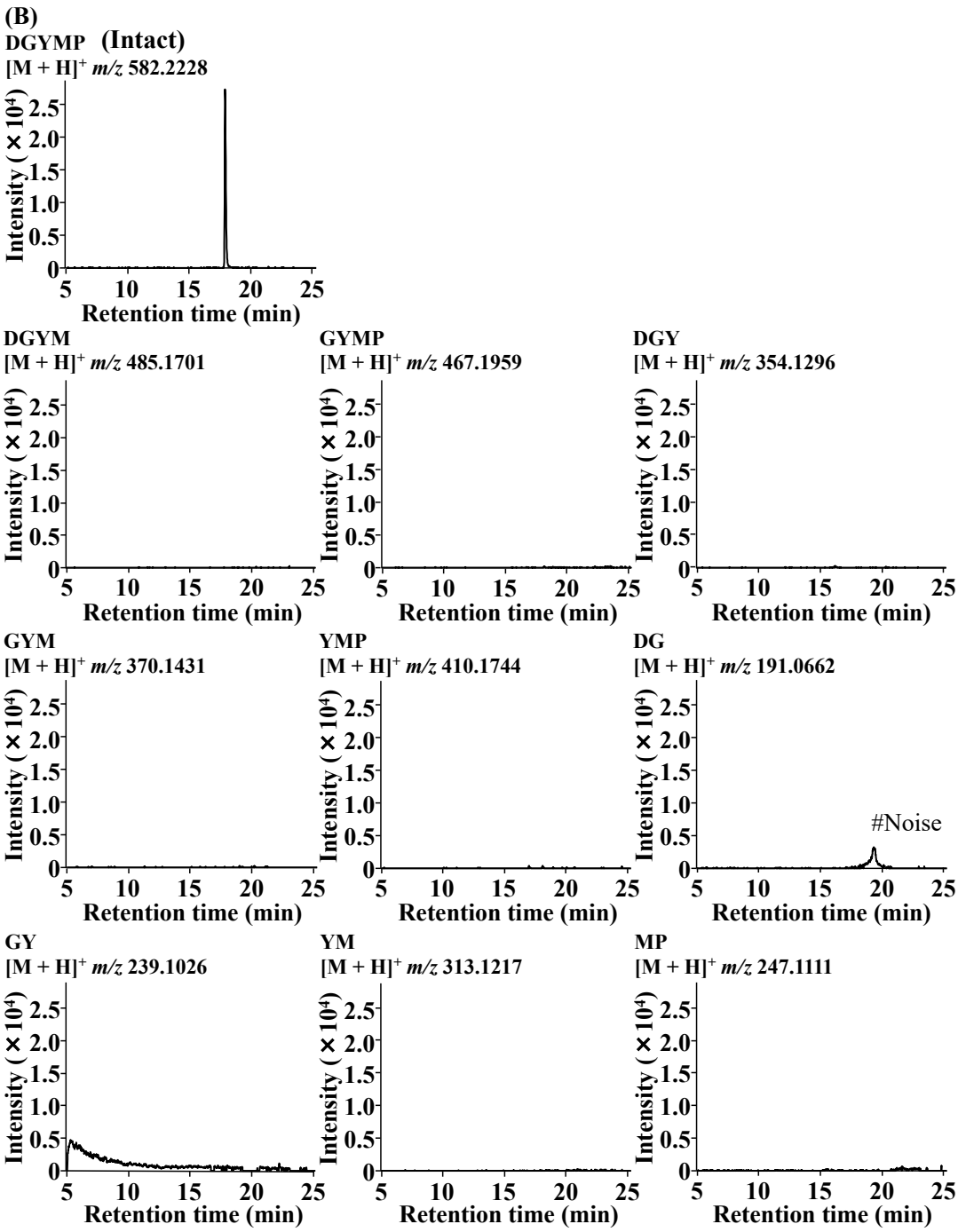

Figure 3-4 (continued). (B) Typical LC-ESI-TOF/MS EICs of peptide degradation fragments after 60 min-transport of DGYMP across Caco-2 cell monolayers. Intact DGYMP was detected, while no peptide fragments were detected in basolateral solutions.

3.2. Transport routes of Cblin pentapeptides in Caco-2 cell monolayers

Transport routes of Cblin oligopeptides were investigated. The involvement of PepT1 was studied by performing competitive transport experiments of the peptides with Gly-Sar (10 mmol/L), a PepT1 substrate [126]. As shown in Figure 3-5, the transports of DGpYMP and DGYMP were not affected in the presence of Gly-Sar, indicating that PepT1 was not involved in the transport of the two peptides across Caco-2 cell monolayers. PepT1 exhibits broad specificity and can recognize a wide variety of di-/tripeptides and peptidomimetic drugs [6, 132]. Meanwhile, crystal structure study of PepT1 revealed that with a binding cavity of approximately 13 × 12 × 11 Å, it could only recognize and transport di-/tripeptides, while could be sterically restrictive for longer peptides [133]. In accordance with these findings, the present results demonstrated that PepT1 is not involved in the transport of Cblin peptides, which are of pentapeptide sizes.

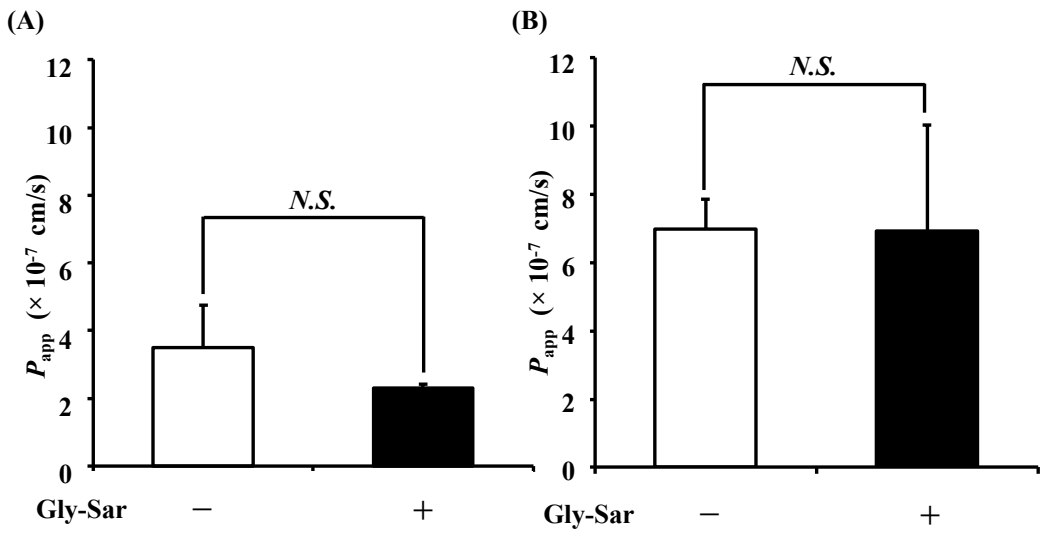

Figure 3-5. Effect of Gly-Sar on the transport of DGpYMP (A) and DGYMP (B) across Caco-2 cell monolayers. Transport experiments of 1 mmol/L DGpYMP and DGYMP in the presence or absence of 10 mmol/L Gly-Sar were performed. After 60 min-transport, the basolateral solution samples were analyzed by LC-TOF/MS and P_{app} values were calculated. Values are expressed as the mean ± SEM (n = 4 ~ 6). Statistical difference between two groups were analyzed by Student's *t*-test. *N.S.*, not significant.

Then involvement of passive diffusion via paracellular TJ was investigated by treating Caco-2 cell monolayers using a TJ opener cytochalasin D [127]. The TEER of Caco-2 cell monolayers decreased significantly after cytochalasin D treatment compared to non-treated monolayers. Transport (P_{app}) of the two peptides was enhanced by cytochalasin D as shown in Figure 3-6. These results suggested that Cblin pentapeptides DGpYMP and DGYMP could penetrate Caco-2 cell monolayers in their intact peptide forms via paracellular TJ. Indeed, paracellular passive diffusion via TJ has been reported to be a predominant transport route for oligopeptides with more than three amino acid residues [19], including pentapeptides IWHHT [30], GPRGF [42], HLPLP [48], VLPVP [49], QIGLF [51], RVPSL [52], GYYPT [53], YPISL [53], YFCLT [54], as well as the model pentapeptide GSSSS [117].

There still could be other routes that are involved in the transport of oligopeptides. For example, transcytosis is reported to be the transport route of a decapeptide YWDHNNPQIR [77] and a 17-residue peptide β-casein (193 – 209) [79], probably owing to their large sizes and hydrophobic properties. In addition, recently, Chothe et al. [134] reported that there is evidence for the existence of broad-specificity oligopeptide transporters that can transport peptides of more than three amino acid residues in Caco-2 cells. However, such transport systems are still not

clarified on a molecular level. Although large remains unknown regarding the cellular uptake and transport of oligopeptides, such oligopeptide transport systems suggested that oligopeptides could be uptaken into cells to elicit their potential bioactivities. Moreover, it is suggested that there could be other routes for the transport of oligopeptides that work in parellel with passive diffusion via TJ, as seen in the transport of di-/tripeptides [135].

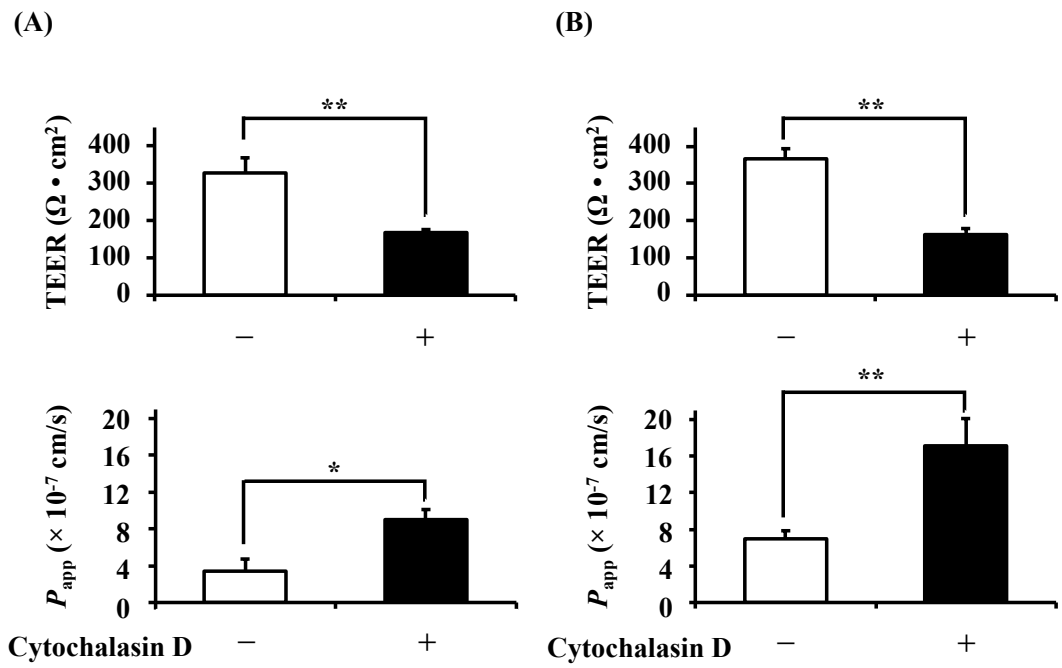

Figure 3-6. Effect of cytochalasin D on the TEER of Caco-2 cell monolayers and transport of DGpYMP (A) and DGYMP (B). Caco-2 cell monolayers were treated with or without 0.5 μg/mL cytochalasin D for 30 min. TEER values were recorded after the treatments. Transport experiments of 1 mmol/L DGpYMP and DGYMP in Caco-2 cell monolayers with or without cytochalasin D treatment. After 60 min-transport, the basolateral solution samples were analyzed by LC-TOF/MS and P_{app} values were calculated. Values are expressed as the mean ± SEM (n = 4 ~ 6). Statistical difference between two groups were analyzed by Student's *t*-test. **p* < 0.05, ***p* < 0.01.

3.3. Absorption and metabolism of Cblin pentaopeptides in SD rats

Single oral administration experiments to SD rats were conducted to evaluate the absorption of DGYMP into rat blood circulation. A single dosage of 100 mg/kg-B.W. of DGYMP was given to each rat using oral gavage. Blood was sampled from the tail vein at 0, 15, 30, 45, and 60 min. Figure 3-7 shows the typical time – intensity EICs of DGYMP from 0 to 60 min. No peak corresponding to DGYMP (*m/z* 582.2228) was detected at 0 min. As soon as 15 min after administration, DGYMP was detected in rat plasma. The signal intensity of DGYMP decreased thereafter, but was detected at all time points through 60 min. These results indicate that the Caco-2 cell transportable pentapeptide DGYMP could be absorbed in its intact peptide form into rat blood circulation. Although di-/tripeptides have been demonstrated to be absorbable upon oral administration [10, 15], large remains unknown regarding the oral bioavailability of longer oligopeptides. In previous studies, we have demonstrated that a model pentapeptide GSSSS with *N*-methylated peptide bonds and consequently resistance against enzymatic degradation could be absorbed into rat blood circulation [125]. In addition, an anti-hypertensive pentapeptide HLPLP and an anti-oxidative nonapeptide WDHHAPQLR were also demonstrated to be absorbable [76, 136]. Together with these studies, the results of the current study furtherly confirmed that oligopeptides with more than three amino acid residues could also be absorbed into blood circulation upon oral intake. It should be noted that for both HLPLP and WDHHAPQLR,

peptide fragments were identified, suggesting that oligopeptides might be degraded during absorption process [76, 136]. Therefore, the metabolism of DGYMP was investigated.

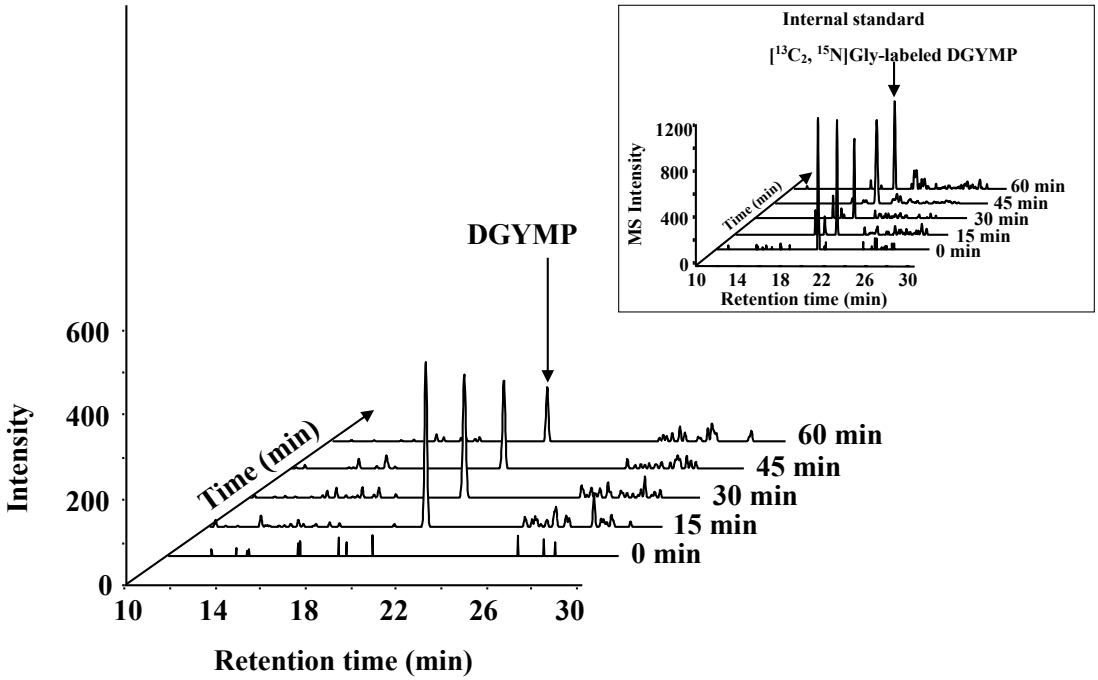

Figure 3-7. Typical stacked LC-ESI-TOF/MS intensity – time EICs of DGYMP ($[M + H]^+$ *m/z* 582.2228) in rat plasma at 0, 15, 30, 45, and 60 min after a single oral administration of 100 mg/kg-B.W. DGYMP to 8-week-old SD rats. Plasma samples were collected from the tail vein and analyzed by LC-ESI-TOF/MS. Corresponding EICs of internal standards ($[^{13}C_2, ^{15}N]$-Gly labeled DGYMP, $[M + H]^+$ *m/z* 585.2228) are shown in the box.

Peptide fragments of DGYMP were screened as a function of *m/z* value. A dipeptide metabolite MP (247.1111 *m/z*) and a tetrapeptide metabolite GYMP (467.1959 *m/z*) were detected, and their typical EICs are shown in Figure 3-8. Although no peptide metabolites were found in *in vitro* Caco-2 studies, DGYMP underwent *in vivo* degradation during the absorption process in SD rat studies, probably in the rat small intestine by exopeptidases and aminopeptidases expressed at the brush border membrane [136]. An anti-hypertensive pentapeptide HLPLP that was demonstrated to be resistant to degradation *in vitro* was also found to be degraded to form LPLP and HLPL *in vivo* [48, 137]. In addition, an anti-oxidative nonapeptide WDHHAPQLR was reported to be metabolized. Interestingly, the fragments of WDHHAPQLR were also demonstrated to be involved in its anti-oxidative property *in vivo* [76]. In this study, peptide fragments GYMP and MP were identified in plasma samples. It has been reported that tyrosine-containing peptide fragments or analogues such as GpYM, DIYNP, and DFYNP might also suppress Cbl-b mediated ubiquitination *in vitro* [138, 139]. Although further investigation is still needed regarding their bioactivity, tyrosine-containing metabolic peptide fragments such as GYMP might contribute to the muscle atrophy preventive effect [83] of Cblin oligopeptides.

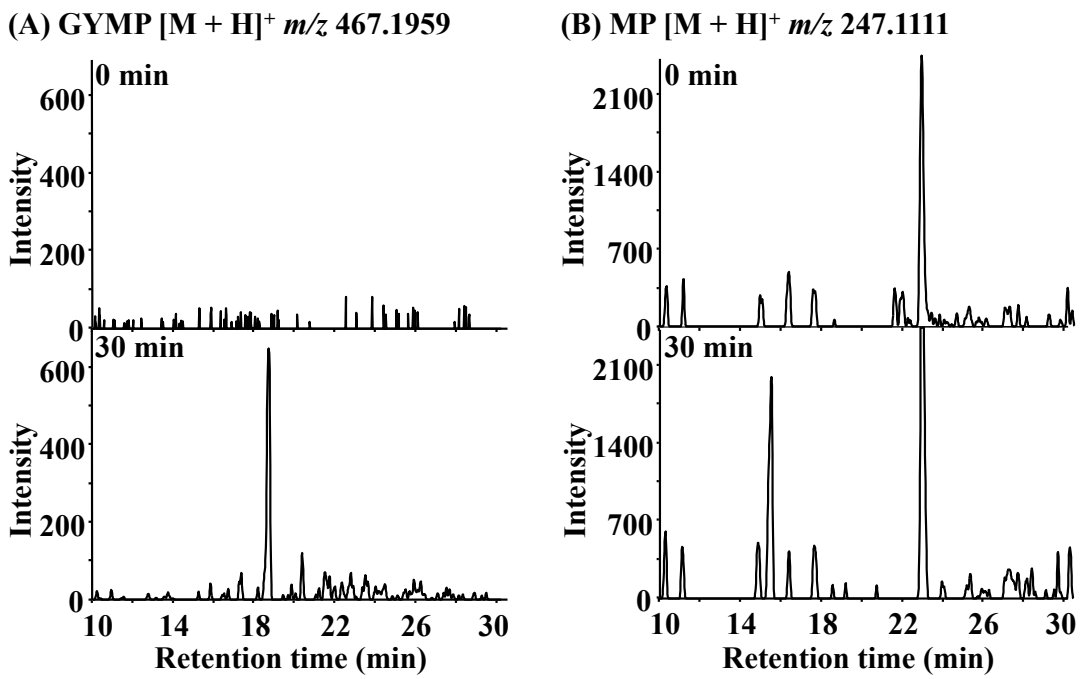

Figure 3-8. (A) Typical LC-ESI-TOF/MS EICs of peptide metabolites GYMP ($[M + H]^+$ *m/z* 467.1959) and (B) MP ($[M + H]^+$ *m/z* 247.1111) of DGYMP in rat plasma after a single oral administration of 100 mg/kg-B.W. DGYMP to 8-week-old SD rats.

3.4. Pharmacokinetics of Cblin oligopeptides

As an internal standard, [$^{13}C_2$, ^{15}N] Gly-labeled DGYMP was spiked to a final concentration of 50 pmol/mL to plasma samples to determine the plasma concentration of absorbed DGYMP by the internal calibration method. The pharmacokinetic parameters of DGYMP are summarized in Table 3-1. As shown in Figure 3-9, the plasma concentration peaked at 15 min (C_{max}: 2.78 ± 0.17 pmol/mL), and then decreased over the next 45 min. An ACE inhibitory dipeptide VY was found to be accumulated into tissues and organs such as aorta, heart, liver, long, and kidney after oral administration [95]. The fast t_{max} and rapid disappearance of DGYMP suggested that it could be distributed and accumulated. However, still further investigation is required. The area under the plasma concentration curve ($AUC_{0\text{-}60\ min}$) was calculated to be 100.35 ± 23.40 pmol·min/mL-plasma. Val-Tyr was absorbed into rat plasma to a C_{max} of 4.11 ± 1.13 pmol/mL-plasma [80]. Moreover, C_{max} values of other small bioactive di-/tripeptides including WH, LY, MY, VPP, IPP, and LPP are also reported to be at pmol/mL order by mg level dosages [24, 80, 140]. Regarding the *in vivo* absorption of oligopeptides of more than three amino acid residues upon oral administration, a pentapeptide HLPLP a nonapeptide WDHHAPQLR were reported to be absorbable to pmol/mL levels in rat models [76, 136]. The C_{max} of DGYMP was comparable to these reported

oligopeptides. These results indicated that oligopeptides with more than 3 amino acid residues could cross the small intestinal barrier and be absorbed into rat blood circulation, providing evidence for their potential biological functions.

Table 3-1. Pharmacokinetic parameters after oral administration of 100 mg/kg-B.W. DGYMP to 8-week-old SD rats.

Pharmacokinetic parameters	
C_{max} (pmol/mL-plasma)	2.78 ± 0.17
t_{max} (min)	15
$AUC_{0-60\ min}$ (pmol·min/mL-plasma)	100.35 ± 24.30
$t_{1/2}$ (min)	28

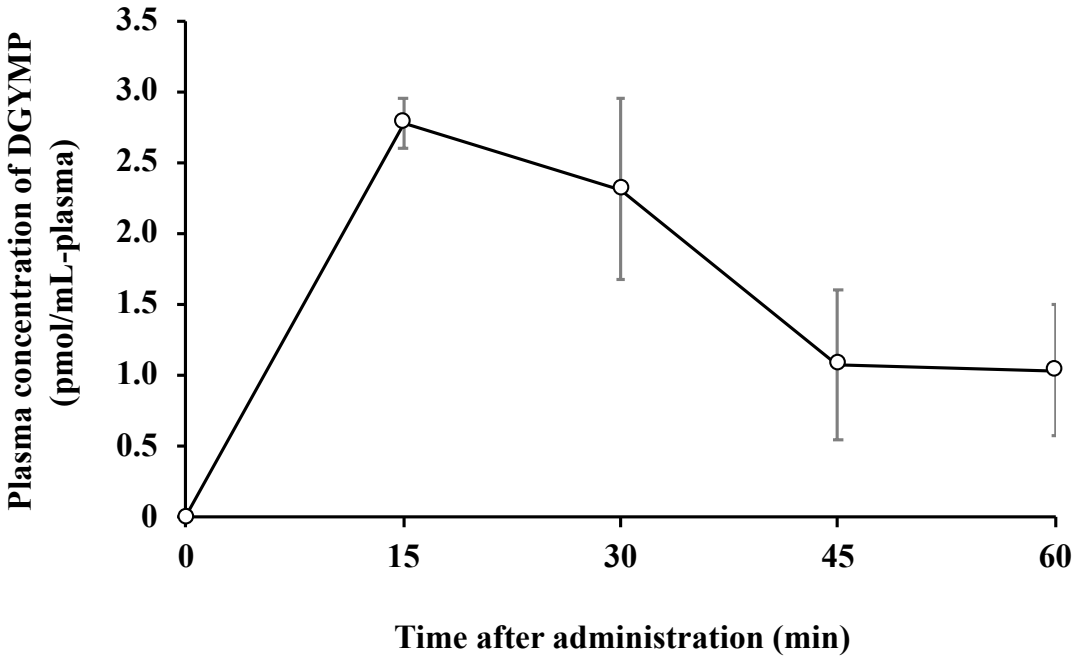

Figure 3-9. Time course plasma concentration of DGYMP after a single oral administration of 100 mg/kg-B.W. to 8-week-old SD rats. Concentrations were calculated based on the LC-ESI-TOF/MS analysis by the internal calibration method. Values are expressed as the mean ± SEM (n = 5).

In previous studies, a series of model di- to pentapeptides based on the structure of GS has been constructed [117]. It is reported that for these model peptides, the absorption was dependent on chain length that GS > GSS > GSSS > GSSSS both *in vitro* and *in vivo* [117, 125]. However, in the current study, although DGYMP showed lower P_{app} in *in vitro* Caco-2 cell studies than di-/tripeptides such as VY [22] and WH [24], no such relationship was observed between the absorption of DGYMP with other reported di-/tripeptides and longer peptides *in vivo*. This could be caused by the relatively lower degradation resistance of the above bioactive peptides compared to GS model peptides. Indeed, the reported pmol/mL level plasma concentration of the above bioactive peptides was also much lower than GS model peptides that were absorbed to nmol/mL plasma concentrations in rats [125]. These results suggested that degradation resistance is an important factor that affects oral bioavailability of oligopeptides. Chemical modification such as cyclization and methylation has been applied to increase stability of peptide therapeutics [141]. As for food, although large remains unclear at the current stage, macronutrients such as fibers and proteins may also interact and impact the systemic availability of oligopeptides [140].

4. Summary

In **Chapter III**, the intestinal absorption behavior of Cblin peptides that could potentially prevent disuse muscle atrophy was investigated using *in vitro* Caco-2 cells and *in vivo* SD rats. In conclusion, both DGpYMP and DGYMP showed appropriate transport across Caco-2 cell monolayers, while passive diffusion via paracellular TJ was demonstrated to be the main transport route involved. DGpYMP was partly dephosphorylated to generate DGYMP during Caco-2 transport. Besides that, no metabolic fragments were detected in Caco-2 transport studies from DGpYMP and DGYMP. Single oral administration of DGYMP to SD rats showed that while a part of DGYMP was degraded and absorbed as peptide fragments, DGYMP could be absorbed into rat blood circulation in its intact peptide form to pmol/mL level (Figure 3-10). These results indicate that Cblin peptides with more than three amino acid residues could also be absorbed and could potentially elicit bioactivity *in vivo*. Although more is to be investigated regarding the systemic bioavailability of Cblin peptides upon oral intake, it is speculated that DGYMP or its functional fragments could reach muscle cells and play a role in the prevention of disuse muscle atrophy.

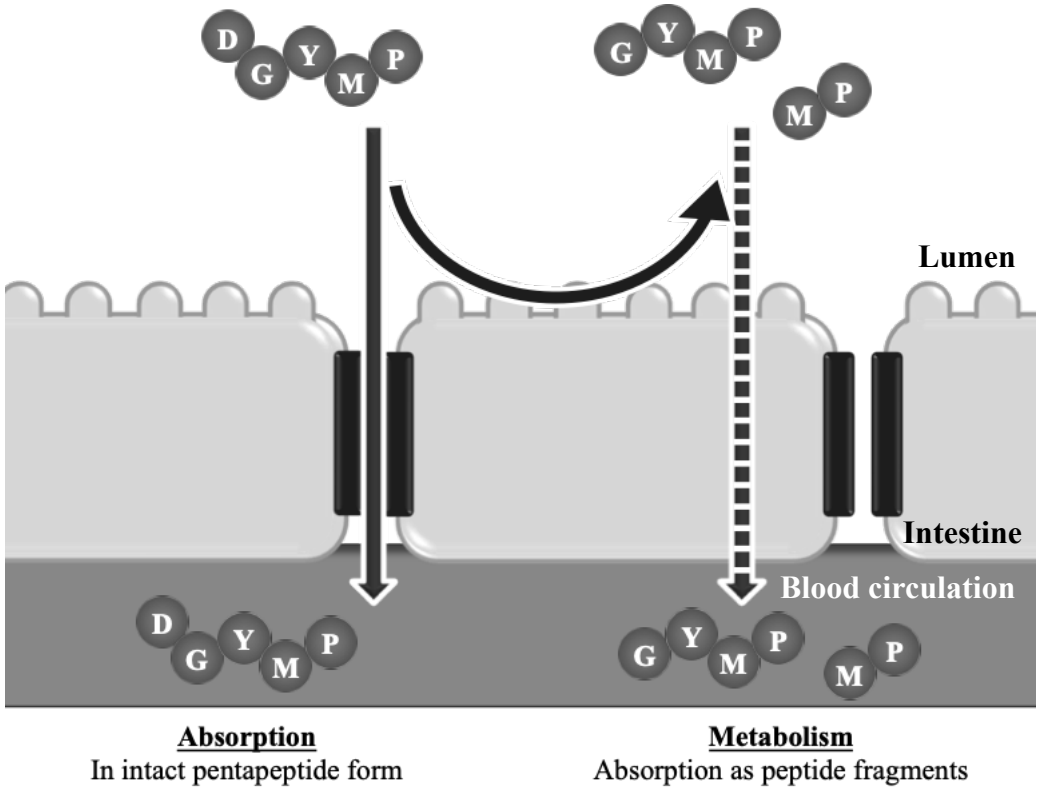

Figure 3-10. Intestinal absorption of DGYMP.

Chapter IV

Conclusion

Food derived short peptides (2 – 20 amino acid residues) have widely received attention on their potential biological functions to prevent lifestyle related diseases [1]. Upon oral intake, such bioactive oligopeptides need to be absorbed into blood circulation via the small intestinal barrier. Therefore, knowledge on the intestinal absorption behavior is crucial for the understanding of the physiological functions of such oligopeptides in living organisms. While the intestinal absorption of di-/tripeptides have been intensively studied, the absorption of longer oligopeptides, which are gaining focus in recent years, is still unclear. To investigate the intestinal absorption behavior of oligopeptides, ESI-MS with high sensitivity and selectivity is considered as an essential tool. Therefore, the ESI-MS detection characteristics of oligopeptides was investigated. Then LC-ESI-MS was used to investigate the *in vitro* and *in*

vivo intestinal absorption of Cblin pentapeptides using Caco-2 cells and SD rats.

Chapter II Investigation of the electrospray ionization detection characteristics of synthetic oligopeptides with chemical derivatization

The ESI-MS detection of a series of synthetic di- to pentapeptides consisting of Gly and Sar was investigated coupled with four amine derivatization reagents, namely, APDS, TNBS, Cou, and NDA, in **Chapter II**. Standard and chemically modified oligopeptides at a concentration of 0.5 μmol/L was analyzed by using LC-ESI-TOF/MS and the relations between MS signal intensity and peptide chain length, log *P*, and CMA, respectively, were evaluated. As a result, all 40 targeted standard and chemically modified oligopeptides were detected by LC-ESI-TOF/MS. In general, chemical derivatization reagents induced greater MS intensity increase to di- and tripeptides than to longer peptides. A moderate correlation was observed between MS signal intensity and log *P* overall but increase in hydrophobicity did not lead to increase in MS signal intensity, especially for longer tetra-/pentapeptides. Meanwhile, a bell-shaped trend between MS signal intensity and molecular surface area was observed, with an optimum of 250 – 300 $Å^2$.

Consequently, it was demonstrated that the size of a molecule was related with its ESI detection characteristics. While addition of hydrophobicity tags was able to increase the MS signal intensity of small amines and di-/tripeptides, it might be less advantageous for longer peptides.

Chapter III Investigation of the intestinal absorption behavior of Cblin peptides in Caco-2 cells and Sprague Dawley rats

The intestinal absorption behavior of Cblin peptides DGpYMP and DGYMP was investigated in **Chapter III**. Cblin peptides DGpYMP and DGYMP are pentapeptides that could potentially prevent disuse muscle atrophy. Caco-2 cell monolayer transport experiments and single oral administration experiments to SD rats (8-week-old) were conducted and samples were analyzed using LC-ESI-TOF/MS. As a result of *in vitro* Caco-2 cell monolayer transport experiments, it was demonstrated that both peptides could penetrate Caco-2 cell monolayers in their intact peptide forms. The P_{app} was 3.5 ± 1.2 cm/s for DGpYMP and 7.0 ± 0.8 cm/s for DGYMP. A screening of peptide metabolites showed that DGpYMP was partly dephosphorylated to generate DGYMP. Meanwhile, no other peptide fragments were detected from the transport of DGpYMP and

DGYMP. In transport route studies, it was demonstrated that PepT1 was not involved in the transport of the two peptides, while passive diffusion via paracellular TJ could be the major route involved. Subsequently, single oral administration of 100 mg/kg-B.W. DGYMP was conducted. It was demonstrated that the pentapeptide could be absorbed in its intact peptide form to a C_{max} of 2.78 ± 0.17 pmol/mL-plasma at 15 min after administration (t_{max}). The $AUC_{0-60\ min}$ was 100.35 ± 23.40 pmol·min/mL-plasma and the $t_{1/2}$ was 28 min. Moreover, peptide fragments GYMP and MP were also detected in rat plasma.

In conclusion, using ESI-MS as a quantitative tool, this study demonstrated that Cblin pentapeptides could cross small intestinal barrier and reach blood circulation. These results suggested that longer oligopeptides with more than tripeptide lengths could be absorbed and potentially elicit bioactivity upon oral intake.

References

[1] Iwaniak, A.; Darewicz, M.; Minkiewicz, P. Peptides derived from foods as supportive diet components in the prevention of metabolic syndrome. *Compr. Rev. Food Sci. Food Saf.* **2018**, *17* (1), 63–81.

[2] Iwatani, S.; Yamamoto, N. Functional food products in Japan: A review. *Food Sci. Hum. Wellness* **2019**, *8* (2), 96–101.

[3] Shimizu, M. History and current status of functional food regulations in Japan. In *Nutraceutical and Functional Food Regulations in the United States and around the World. Third Edit.*; Elsevier: Amsterdam, the Netherlands, 2019; 337-344.

[4] Foltz, M.; Van Der Pijl, P. C.; Duchateau, G. S. M. J. E. Current *in vitro* testing of bioactive peptides is not valuable. *J. Nutr.* **2010**, *140* (1), 117–118.

[5] Turner, J. R. Intestinal mucosal barrier function in health and disease. *Nat. Rev. Immunol.* **2009**, *9* (11), 799–809.

[6] Fei, Y.J.; Kanai, Y.; Nussberger, S.; Ganapathy, V.; Leibach, F. H.; Romero, M. F.; Singh, S. K.; Boron, W. F.; Hediger, M. A. Expression cloning of a mammalian proton-coupled oligopeptide transporter. *Nature* **1994**, *368* (6471), 563–566.

[7] Fei, Y. J.; Sugawara, M.; Liu, J. C.; Li, H. W.; Ganapathy, V.; Ganapathy, M. E.; Leibach, F. H. cDNA structure, genomic organization, and promoter analysis of the mouse intestinal peptide transporter PEPT1. *Biochim. Biophys. Acta - Gene Struct. Expr.* **2000**, *1492* (1), 145–154.

[8] Liang, R.; Fei, Y. J.; Prasad, P. D.; Ramamoorthy, S.; Han, H.; Yang-Feng, T. L.; Hediger, M. A.; Ganapathy, V.; Leibach, F. H. Human intestinal H^+/peptide cotransporter. Cloning, functional expression, and chromosomal localization. *J. Biol. Chem.* **1995**, *270* (12), 6456–6463.

[9] Matsui, T.; Zhu, X. L.; Watanabe, K.; Tanaka, K.; Kusano, Y.; Matsumoto, K. Combined administration of captopril with an antihypertensive Val-Tyr di-peptide to spontaneously hypertensive rats attenuates the blood pressure lowering effect. *Life Sci.* **2006**, *79* (26), 2492–2498.

[10] Matsui, T.; Tamaya, K.; Seki, E.; Osajima, K.; Matsumoto, K.; Kawasaki, T. Absorption of Val-Tyr with *in vitro* angiotensin I-converting enzyme inhibitory activity into the circulating blood system of mild hypertensive subjects. *Biol. Pharm. Bull.* **2002**, *25* (9), 1228–1230.

[11] Kawasaki, T.; Seki, E.; Osajima, K.; Yoshida, M.; Asada, K.; Matsui, T.; Osajima, Y. Antihypertensive effect of valyl-tyrosine, a short chain peptide derived from sardine muscle hydrolyzate, on mild hypertensive subjects. *J. Hum. Hypertens.* **2000**, *14* (8), 519–523.

[12] Li, S.; Bu, T.; Zheng, J.; Liu, L.; He, G.; Wu, J. Preparation, bioavailability, and mechanism of emerging activities of Ile-Pro-Pro and Val-Pro-Pro. *Compr. Rev. Food Sci. Food Saf.* **2019**, *18* (4), 1097–1110.

[13] Fekete, Á. A.; Ian Givens, D.; Lovegrove, J. A. Casein-derived lactotripeptides reduce systolic and diastolic blood pressure in a meta-analysis of randomised clinical trials. *Nutrients* **2015**, *7* (1), 659–681.

[14] Satake, M.; Enjoh, M.; Nakamura, Y.; Takano, T.; Kawamura, Y.; Arai, S.; Shimizu, M. Transepithelial transport of the bioactive

tripeptide, Val-Pro-Pro, in human intestinal Caco-2 cell monolayers. *Biosci. Biotechnol. Biochem.* **2002**, *66* (2), 378–384.

[15] Foltz, M.; Meynen, E. E.; Bianco, V.; Van Platerink, C.; Koning, T. M. M. G.; Kloek, J. Angiotensin converting enzyme inhibitory peptides from a lactotripeptide-enriched milk beverage are absorbed intact into the circulation. *J. Nutr.* **2007**, *137* (4), 953–958.

[16] Engle, M. J.; Goetz, G. S.; Alpers, D. H. Caco-2 cells express a combination of colonocyte and enterocyte phenotypes. *J. Cell. Physiol.* **1998**, *174* (3), 362–369.

[17] Sambuy, Y.; De Angelis, I.; Ranaldi, G.; Scarino, M. L.; Stammati, A.; Zucco, F. The Caco-2 cell line as a model of the intestinal barrier: Influence of cell and culture-related factors on Caco-2 cell functional characteristics. *Cell Biol. Toxicol.* **2005**, *21* (1), 1–26.

[18] Hidalgo, I. J.; Raub, T. J.; Borchardt, R. T. Characterization of the human colon carcinoma cell line (Caco-2) as a model system for intestinal epithelial permeability. *Gastroenterology* **1989**, *96* (3), 736–749.

[19] Shen, W.; Matsui, T. Current knowledge of intestinal absorption of bioactive peptides. *Food Funct.* **2017**, *8* (12), 4306–4314.

[20] Zhu, X. L.; Watanabe, K.; Shiraishi, K.; Ueki, T.; Noda, Y.; Matsui, T.; Matsumoto, K. Identification of ACE-inhibitory peptides in salt-free soy sauce that are transportable across Caco-2 cell monolayers. *Peptides* **2008**, *29* (3), 338–344.

[21] Pentzien, A. K.; Meisel, H. Transepithelial transport and stability in blood serum of angiotensin-I-converting enzyme inhibitory dipeptides. *Zeitschrift für Naturforsch. - Sect. C J. Biosci.* **2008**, *63* (5–6), 451–459.

[22] Takeda, J.; Park, H. Y.; Kunitake, Y.; Yoshiura, K.; Matsui, T. Theaflavins, dimeric catechins, inhibit peptide transport across Caco-2 cell monolayers via down-regulation of AMP-activated protein kinase-mediated peptide transporter PEPT1. *Food Chem.* **2013**, *138* (4), 2140–2145.

[23] Fernández-Musoles, R.; Salom, J. B.; Castelló-Ruiz, M.; Contreras, M. del M.; Recio, I.; Manzanares, P. Bioavailability of antihypertensive lactoferricin B-derived peptides: Transepithelial transport and resistance to intestinal and plasma peptidases. *Int. Dairy J.* **2013**, *32* (2), 169–174.

[24] Tanaka, M.; Hong, S. M.; Akiyama, S.; Hu, Q. Q.; Matsui, T. Visualized absorption of anti-atherosclerotic dipeptide, Trp-His, in

Sprague-Dawley rats by LC-MS and MALDI-MS imaging analyses. *Mol. Nutr. Food Res.* **2015**, *59* (8), 1541–1549.

[25] Osborne, S.; Chen, W.; Addepalli, R.; Colgrave, M.; Singh, T.; Tran, C.; Day, L. *In vitro* transport and satiety of a beta-lactoglobulin dipeptide and beta-casomorphin-7 and its metabolites. *Food Funct.* **2014**, *5* (11), 2706–2718.

[26] Sontakke, S. B.; Jung, J. H.; Piao, Z.; Chung, H. J. Orally available collagen tripeptide: enzymatic stability, intestinal permeability, and absorption of Gly-Pro-Hyp and Pro-Hyp. *J. Agric. Food Chem.* **2016**, *64* (38), 7127–7133.

[27] Yang, Y. J.; He, H. Y.; Wang, F. Z.; Ju, X. R.; Yuan, J.; Wang, L. F.; Aluko, R. E.; He, R. Transport of angiotensin converting enzyme and renin dual inhibitory peptides LY, RALP and TF across Caco-2 cell monolayers. *J. Funct. Foods* **2017**, *35*, 303–314.

[28] Lacroix, I. M. E.; Chen, X. M.; Kitts, D. D.; Li-Chan, E. C. Y. Investigation into the bioavailability of milk protein-derived peptides with dipeptidyl-peptidase IV inhibitory activity using Caco-2 cell monolayers. *Food Funct.* **2017**, *8* (2), 701–709.

[29] Khueychai, S.; Jangpromma, N.; Choowongkomon, K.; Joompang, A.; Daduang, S.; Vesaratchavest, M.; Payoungkiattikun, W.;

Tachibana, S.; Klaynongsruang, S. A novel ACE inhibitory peptide derived from alkaline hydrolysis of ostrich (*Struthio camelus*) egg white ovalbumin. *Process Biochem.* **2018**, *73* (July), 235–245.

[30] Fan, H.; Xu, Q.; Hong, H.; Wu, J. Stability and transport of spent hen-derived ACE-inhibitory peptides IWHHT, IWH, and IW in human intestinal Caco-2 cell monolayers. *J. Agric. Food Chem.* **2018**, *66* (43), 11347–11354.

[31] Foltz, M.; Cerstiaens, A.; van Meensel, A.; Mols, R.; van der Pijl, P. C.; Duchateau, G. S. M. J. E.; Augustijns, P. The angiotensin converting enzyme inhibitory tripeptides Ile-Pro-Pro and Val-Pro-Pro show increasing permeabilities with increasing physiological relevance of absorption models. *Peptides* **2008**, *29* (8), 1312–1320.

[32] Miguel, M.; Dávalos, A.; Manso, M. A.; De La Peña, G.; Lasunción, M. A.; López-Fandiño, R. Transepithelial transport across Caco-2 cell monolayers of antihypertensive egg-derived peptides. PepT1-mediated flux of Tyr-Pro-Ile. *Mol. Nutr. Food Res.* **2008**, *52* (12), 1507–1513.

[33] Kovacs-Nolan, J.; Zhang, H.; Ibuki, M.; Nakamori, T.; Yoshiura, K.; Turner, P. V.; Matsui, T.; Mine, Y. The PepT1-transportable soy

tripeptide VPY reduces intestinal inflammation. *Biochim. Biophys. Acta - Gen. Subj.* **2012**, *1820* (11), 1753–1763.

[34] Bejjani, S.; Wu, J. Transport of IRW, an ovotransferrin-derived antihypertensive peptide, in human intestinal epithelial Caco-2 cells. *J. Agric. Food Chem.* **2013**, *61* (7), 1487–1492.

[35] Gleeson, J. P.; Brayden, D. J.; Ryan, S. M. Evaluation of PepT1 transport of food-derived antihypertensive peptides, Ile-Pro-Pro and Leu-Lys-Pro using *in vitro*, *ex vivo* and *in vivo* transport models. *Eur. J. Pharm. Biopharm.* **2017**, *115*, 276–284.

[36] Lin, Q.; Xu, Q.; Bai, J.; Wu, W.; Hong, H.; Wu, J. Transport of soybean protein-derived antihypertensive peptide LSW across Caco-2 monolayers. *J. Funct. Foods* **2017**, *39* (September), 96–102.

[37] Xu, Q.; Fan, H.; Yu, W.; Hong, H.; Wu, J. Transport study of egg-derived antihypertensive peptides (LKP and IQW) using Caco-2 and HT29 coculture monolayers. *J. Agric. Food Chem.* **2017**, *65* (34), 7406–7414.

[38] Sowmya, K.; Mala, D.; Bhat, M. I.; Kumar, N.; Bajaj, R. K.; Kapila, S.; Kapila, R. Bio-accessible milk casein derived tripeptide (LLY) mediates overlapping anti-inflammatory and anti-oxidative effects

under cellular (Caco-2) and *in vivo* milieu. *J. Nutr. Biochem.* **2018**, *62*, 167–180.

[39] He, Y. Y.; Li, T. T.; Chen, J. X.; She, X. X.; Ren, D. F.; Lu, J. Transport of ACE inhibitory peptides Ile-Gln-Pro and Val-Glu-Pro derived from *Spirulina platensis* across Caco-2 monolayers. *J. Food Sci.* **2018**, *83* (10), 2586–2592.

[40] Li, Y.; Wang, B.; Li, B. The *in vitro* bioavailability of anti-platelet peptides in collagen hydrolysate from silver carp (*Hypophthalmichthys molitrix*) skin. *J. Food Biochem.* **2020**, *44* (6), e13226.

[41] Shimizu, M.; Tsunogai, M.; Arai, S. Transepithelial transport of oligopeptides in the human intestinal cell, Caco-2. *Peptides* **1997**, *18* (5), 681–687.

[42] Fu, Y.; Young, J. F.; Rasmussen, M. K.; Dalsgaard, T. K.; Lametsch, R.; Aluko, R. E.; Therkildsen, M. Angiotensin I-converting enzyme-inhibitory peptides from bovine collagen: Insights into inhibitory mechanism and transepithelial transport. *Food Res. Int.* **2016**, *89*, 373–381.

[43] Li, Y.; Zhao, J.; Liu, X.; Xia, X.; Wang, Y.; Zhou, J. Transport of a novel angiotensin-I-converting enzyme inhibitory peptide Ala-His-

Leu-Leu across human intestinal epithelial Caco-2 cells. *J. Med. Food* **2017**, *20* (3), 243–250.

[44] Xing, L.; Liu, R.; Tang, C.; Pereira, J.; Zhou, G.; Zhang, W. The antioxidant activity and transcellular pathway of Asp-Leu-Glu-Glu in a Caco-2 cell monolayer. *Int. J. Food Sci. Technol.* **2018**, *53* (10), 2405–2414.

[45] Sangsawad, P.; Choowongkomon, K.; Kitts, D. D.; Chen, X. M.; Li-Chan, E. C. Y.; Yongsawatdigul, J. Transepithelial transport and structural changes of chicken angiotensin I-converting enzyme (ACE) inhibitory peptides through Caco-2 cell monolayers. *J. Funct. Foods* **2018**, *45* (April), 401–408.

[46] Aiello, G.; Ferruzza, S.; Ranaldi, G.; Sambuy, Y.; Arnoldi, A.; Vistoli, G.; Lammi, C. Behavior of three hypocholesterolemic peptides from soy protein in an intestinal model based on differentiated Caco-2 cell. *J. Funct. Foods* **2018**, *45* (March), 363–370.

[47] Ritian, J.; Teng, X.; Liao, M.; Zhang, L.; Wei, Z.; Meng, R.; Liu, N. Release of dipeptidyl peptidase IV inhibitory peptides from salmon (*Salmo salar*) skin collagen based on digestion–intestinal absorption *in vitro*. *Int. J. Food Sci. Technol.* **2021**, *56* (7), 3507–3518.

[48] Quirós, A.; Dávalos, A.; Lasunción, M. A.; Ramos, M.; Recio, I. Bioavailability of the antihypertensive peptide LHLPLP: Transepithelial flux of HLPLP. *Int. Dairy J.* **2008**, *18* (3), 279–286.

[49] Lei, L.; Sun, H.; Liu, D.; Liu, L.; Li, S. Transport of Val-Leu-Pro-Val-Pro in human intestinal epithelial (Caco-2) cell monolayers. *J. Agric. Food Chem.* **2008**, *56* (10), 3582–3586.

[50] Sienkiewicz-Szłapka, E.; Jarmołowska, B.; Krawczuk, S.; Kostyra, E.; Kostyra, H.; Bielikowicz, K. Transport of bovine milk-derived opioid peptides across a Caco-2 monolayer. *Int. Dairy J.* **2009**, *19* (4), 252–257.

[51] Ding, L.; Zhang, Y.; Jiang, Y.; Wang, L.; Liu, B.; Liu, J. Transport of egg white ACE-inhibitory peptide, Gln-Ile-Gly-Leu-Phe, in human intestinal Caco-2 cell monolayers with cytoprotective effect. *J. Agric. Food Chem.* **2014**, *62* (14), 3177–3182.

[52] Ding, L.; Wang, L.; Zhang, Y.; Liu, J. Transport of antihypertensive peptide RVPSL, ovotransferrin 328 – 332, in human intestinal Caco-2 cell monolayers. *J. Agric. Food Chem.* **2015**, *63* (37), 8143–8150.

[53] Maggioni, M.; Stuknytė, M.; De Luca, P.; Cattaneo, S.; Fiorilli, A.; De Noni, I.; Ferraretto, A. Transport of wheat gluten exorphins A5

and C5 through an *in vitro* model of intestinal epithelium. *Food Res. Int.* **2016**, *88* (Part B), 319–326.

[54] Ding, L.; Wang, L.; Zhang, T.; Yu, Z.; Liu, J. Hydrolysis and transepithelial transport of two corn gluten derived bioactive peptides in human Caco-2 cell monolayers. *Food Res. Int.* **2018**, *106*, 475–480.

[55] Sun, H.; Liu, D.; Li, S.; Qin, Z. Transepithelial transport characteristics of the antihypertensive peptide, Lys-Val-Leu-Pro-Val-Pro, in human intestinal Caco-2 cell monolayers. *Biosci. Biotechnol. Biochem.* **2009**, *73* (2), 293–298.

[56] Gallego, M.; Grootaert, C.; Mora, L.; Aristoy, M. C.; Van Camp, J.; Toldrá, F. Transepithelial transport of dry-cured ham peptides with ACE inhibitory activity through a Caco-2 cell monolayer. *J. Funct. Foods* **2016**, *21*, 388–395.

[57] Ding, L.; Wang, L.; Yu, Z.; Zhang, T.; Liu, J. Digestion and absorption of an egg white ACE-inhibitory peptide in human intestinal Caco-2 cell monolayers. *Int. J. Food Sci. Nutr.* **2016**, *67* (2), 111–116.

[58] Guo, Y.; Gan, J.; Zhu, Q.; Zeng, X.; Sun, Y.; Wu, Z.; Pan, D. Transepithelial transport of milk-derived angiotensin I-converting

enzyme inhibitory peptide with the RLSFNP sequence. *J. Sci. Food Agric.* **2018**, *98* (3), 976–983.

[59] Zhang, C.; Liu, H.; Chen, S.; Luo, Y. Evaluating the effects of IADHFL on inhibiting DPP-IV activity and expression in Caco-2 cells and contributing to the amount of insulin released from INS-1 cells *in vitro*. *Food Funct.* **2018**, *9* (4), 2240–2250.

[60] Tianrui, Z.; Bingtong, L.; Ling, Y.; Liping, S.; Yongliang, Z. ACE inhibitory activity *in vitro* and antihypertensive effect *in vivo* of LSGYGP and its transepithelial transport by Caco-2 cell monolayer. *J. Funct. Foods* **2019**, *61* (January), 103488.

[61] Zhang, T.; Su, M.; Jiang, X.; Xue, Y.; Zhang, J.; Zeng, X.; Wu, Z.; Guo, Y.; Pan, D. Transepithelial transport route and liposome encapsulation of milk-derived ACE-inhibitory peptide Arg-Leu-Ser-Phe-Asn-Pro. *J. Agric. Food Chem.* **2019**, *67* (19), 5544–5551.

[62] Sowmya, K.; Bhat, M. I.; Bajaj, R.; Kapila, S.; Kapila, R. Antioxidative and anti-inflammatory potential with trans-epithelial transport of a buffalo casein-derived hexapeptide (YFYPQL). *Food Biosci.* **2019**, *28* (January), 151–163.

[63] Zhang, H.; Duan, Y.; Feng, Y.; Wang, J. Transepithelial transport characteristics of the cholesterol-lowing soybean peptide, WGAPSL, in Caco-2 cell monolayers. *Molecules* **2019**, *24* (15), 2843.

[64] Lin, K.; Ma, Z.; Ramachandran, M.; De Souza, C.; Han, X.; Zhang, L. ACE inhibitory peptide KYIPIQ derived from yak milk casein induces nitric oxide production in HUVECs and diffuses via a transcellular mechanism in Caco-2 monolayers. *Process Biochem.* **2020**, *99* (August), 103–111.

[65] Hong, H.; Zheng, Y.; Song, S.; Zhang, Y.; Zhang, C.; Liu, J.; Luo, Y. Identification and characterization of DPP-IV inhibitory peptides from silver carp swim bladder hydrolysates. *Food Biosci.* **2020**, *38* (August), 100748.

[66] Dang, Y.; Pei, J.; Hua, Y.; Zhou, T.; Gao, X.; Wang, Y. Transport, *in vivo* antihypertensive effect, and pharmacokinetics of an angiotensin-converting enzyme (ACE) inhibitory peptide LVLPGE. *J. Agric. Food Chem.* **2021**, *69* (7), 2149–2156.

[67] Vermeirssen, V.; Deplancke, B.; Tappenden, K. A.; Van Camp, J.; Gaskins, H. R.; Verstraete, W. Intestinal transport of the lactokinin Ala-Leu-Pro-Met-His-Ile-Arg through a Caco-2 Bbe monolayer. *J. Pept. Sci.* **2002**, *8* (3), 95–100.

[68] Cakir-Kiefer, C.; Miclo, L.; Balandras, F.; Dary, A.; Soligot, C.; Roux, Y. Le. Transport across Caco-2 cell monolayer and sensitivity to hydrolysis of two anxiolytic peptides from α_{s1}-casein, α-casozepine, and α_{s1}-casein-(f91 – 97): Effect of bile salts. *J. Agric. Food Chem.* **2011**, *59* (22), 11956–11965.

[69] Vij, R.; Reddi, S.; Kapila, S.; Kapila, R. Transepithelial transport of milk derived bioactive peptide VLPVPQK. *Food Chem.* **2016**, *190*, 681–688.

[70] Jin, R.; Shang, J.; Teng, X.; Zhang, L.; Liao, M.; Kang, J.; Meng, R.; Wang, D.; Ren, H.; Liu, N. Characterization of DPP-IV inhibitory peptides using an *in vitro* cell culture model of the intestine. *J. Agric. Food Chem.* **2021**, *69* (9), 2711–2718.

[71] Shimizu, K.; Sato, M.; Zhang, Y.; Kouguchi, T.; Takahata, Y.; Morimatsu, F.; Shimizu, M. The bioavailable octapeptide Gly-Ala-Hyp-Gly-Leu-Hyp-Gly-Pro stimulates nitric oxide synthesis in vascular endothelial cells. *J. Agric. Food Chem.* **2010**, *58* (11), 6960–6965.

[72] Fernández-Tomé, S.; Sanchón, J.; Recio, I.; Hernández-Ledesma, B. Transepithelial transport of lunasin and derived peptides: Inhibitory

effects on the gastrointestinal cancer cells viability. *J. Food Compos. Anal.* **2018**, *68*, 101–110.

[73] Sun, L.; Wu, B.; Yan, M.; Hou, H.; Zhuang, Y. Antihypertensive effect *in vivo* of QAGLSPVR and its transepithelial transport through the Caco-2 cell monolayer. *Mar. Drugs* **2019**, *17* (5), 288.

[74] Xu, F.; Mejia, E. G. de; Chen, H.; Rebecca, K.; Pan, M.; He, R.; Yao, Y.; Wang, L.; Ju, X. Assessment of the DPP-IV inhibitory activity of a novel octapeptide derived from rapeseed using Caco-2 cell monolayers and molecular docking analysis. *J. Food Biochem.* **2020**, *44* (10), e13406.

[75] Lammi, C.; Aiello, G.; Bollati, C.; Li, J.; Bartolomei, M.; Ranaldi, G.; Ferruzza, S.; Fassi, E. M. A.; Grazioso, G.; Sambuy, Y.; Arnoldi, A. Trans-epithelial transport, metabolism and biological activity assessment of the multi-target lupin peptide LILPKHSDAD (P5) and its metabolite LPKHSDAD (P5-met). *Nutrients* **2021**, *13* (3), 863.

[76] Xu, F.; Zhang, J.; Wang, Z.; Yao, Y.; Atungulu, G. G.; Ju, X.; Wang, L. Absorption and metabolism of peptide WDHHAPQLR derived from rapeseed protein and inhibition of HUVEC apoptosis under oxidative stress. *J. Agric. Food Chem.* **2018**, *66* (20), 5178–5189.

[77] Xu, F.; Wang, L.; Ju, X.; Zhang, J.; Yin, S.; Shi, J.; He, R.; Yuan, Q. Transepithelial transport of YWDHNNPQIR and its metabolic fate with cytoprotection against oxidative stress in human intestinal Caco-2 cells. *J. Agric. Food Chem.* **2017**, *65* (10), 2056–2065.

[78] Xu, Z.; Chen, H.; Fan, F.; Shi, P.; Cheng, S.; Tu, M.; Ei-Seedi, H. R.; Du, M.; Du, M. Pharmacokinetics and transport of an osteogenic dodecapeptide. *J. Agric. Food Chem.* **2020**, *68* (37), 9961–9967.

[79] Regazzo, D.; Mollé, D.; Gabai, G.; Tomé, D.; Dupont, D.; Leonil, J.; Boutrou, R. The (193 – 209) 17-residues peptide of bovine β-casein is transported through Caco-2 monolayer. *Mol. Nutr. Food Res.* **2010**, *54* (10), 1428–1435.

[80] Nakashima, E. M. N.; Kudo, A.; Iwaihara, Y.; Tanaka, M.; Matsumoto, K.; Matsui, T. Application of ^{13}C stable isotope labeling liquid chromatography-multiple reaction monitoring-tandem mass spectrometry method for determining intact absorption of bioactive dipeptides in rats. *Anal. Biochem.* **2011**, *414* (1), 109–116.

[81] Nakashima, E. M. N.; Qing, H. Q.; Tanaka, M.; Matsui, T. Improved detection of di-peptides by liquid chromatography-tandem mass spectrometry with 2,4,6-trinitrobenzene sulfonate conversion. *Biosci. Biotechnol. Biochem.* **2013**, *77* (10), 2094–2099.

[82] Hashimoto, C.; Iwaihara, Y.; Chen, S. J.; Tanaka, M.; Watanabe, T.; Matsui, T. Highly-sensitive detection of free advanced glycation end-products by liquid chromatography-electrospray ionization-tandem mass spectrometry with 2,4,6-trinitrobenzene sulfonate derivatization. *Anal. Chem.* **2013**, *85* (9), 4289–4295.

[83] Nakao, R.; Hirasaka, K.; Goto, J.; Ishidoh, K.; Yamada, C.; Ohno, A.; Okumura, Y.; Nonaka, I.; Yasutomo, K.; Baldwin, K. M.; Kominami, E.; Higashibata, A.; Nagano, K.; Tanaka, K.; Yasui, N.; Mills, E. M.; Takeda, S.; Nikawa, T. Ubiquitin ligase Cbl-b is a negative regulator for insulin-like growth factor 1 signaling during muscle atrophy caused by unloading. *Mol. Cell. Biol.* **2009**, *29* (17), 4798–4811.

[84] Kawai, N.; Hirasaka, K.; Maeda, T.; Haruna, M.; Shiota, C.; Ochi, A.; Abe, T.; Kohno, S.; Ohno, A.; Teshima-Kondo, S.; Mori, H.; Tanaka, E.; Nikawa, T. Prevention of skeletal muscle atrophy *in vitro* using anti-ubiquitination oligopeptide carried by atelocollagen. *Biochim. Biophys. Acta - Mol. Cell Res.* **2015**, *1853* (5), 873–880.

[85] Ochi, A.; Abe, T.; Nakao, R.; Yamamoto, Y.; Kitahata, K.; Takagi, M.; Hirasaka, K.; Ohno, A.; Teshima-Kondo, S.; Taesik, G.; Choi, I.; Kawamura, T.; Nemoto, H.; Mukai, R.; Terao, J.; Nikawa, T. *N*-myristoylated ubiquitin ligase Cbl-b inhibitor prevents on

glucocorticoid-induced atrophy in mouse skeletal muscle. *Arch. Biochem. Biophys.* **2015**, *570*, 23–31.

[86] Thomason, D. B.; Biggs, R. B.; Booth, F. W. Protein metabolism and beta-myosin heavy-chain mRNA in unweighted soleus muscle. *Am. J. Physiol. Integr. Comp. Physiol.* **1989**, *257* (2), R300–R305.

[87] Tischler, M. E.; Rosenberg, S.; Satarug, S.; Henriksen, E. J.; Kirby, C. R.; Tome, M.; Chase, P. Different mechanisms of increased proteolysis in atrophy induced by denervation or unweighting of rat soleus muscle. *Metabolism* **1990**, *39* (7), 756–763.

[88] Nikawa, T.; Ishidoh, K.; Hirasaka, K.; Ishihara, I.; Ikemoto, M.; Kano, M.; Kominami, E.; Nonaka, I.; Ogawa, T.; Adams, G. R.; Baldwin, K. M.; Yasui, N.; Kishi, K.; Takeda, S. Skeletal muscle gene expression in space-flown rats. *FASEB J.* **2004**, *18* (3), 522–524.

[89] Matsui, T.; Tanaka, M. Antihypertensive peptides and their underlying mechanisms. In *Bioactive Proteins and Peptides as Functional Foods and Nutraceuticals*; Wiley-Blackwell: Oxford, UK, 2010; 43–54.

[90] Shangguan, D.; Zhao, Y.; Han, H.; Zhao, R.; Liu, G. Derivatization and fluorescence detection of amino acids and peptides with 9-

fluorenylmethyl chloroformate on the surface of a solid adsorbent. *Anal. Chem.* **2001**, *73* (9), 2054–2057.

[91] Deantonis, K. M.; Brown, P. R.; Cohen, S. A. High-performance liquid chromatographic analysis of synthetic peptides using derivatization with 6-aminoquinolyl-*N*-hydroxysuccinimidyl carbamate. *Anal. Biochem.* **1994**, *223* (2), 191–197.

[92] Zhu, R.; Kok, W. T. Postcolumn derivatization of peptides with fluorescamine in capillary electrophoresis. *J. Chromatogr. A* **1998**, *814* (1–2), 213–221.

[93] Kang, X.; Xiao, J.; Huang, X.; Gu, Z. Optimization of dansyl derivatization and chromatographic conditions in the determination of neuroactive amino acids of biological samples. *Clin. Chim. Acta* **2006**, *366* (1–2), 352–356.

[94] Matsui, T.; Tamaya, K.; Kawasaki, T.; Osajima, Y. Determination of angiotensin metabolites in human plasma by fluorimetric high-performance liquid chromatography using a heart-cut column-switching technique. *J. Chromatogr. B Biomed. Sci. Appl.* **1999**, *729* (1–2), 89–95.

[95] Matsui, T.; Imamura, M.; Oka, H.; Osajima, K.; Kimoto, K. I.; Kawasaki, T.; Matsumoto, K. Tissue distribution of antihypertensive

dipeptide, Val-Tyr, after its single oral administration to spontaneously hypertensive rats. *J. Pept. Sci.* **2004**, *10* (9), 535–545.

[96] Wilm, M. Principles of electrospray ionization. *Mol. Cell. Proteomics* **2011**, *10* (7), M111.009407.

[97] Iribarne, J. V.; Dziedzic, P. J.; Thomson, B. A. Atmospheric pressure ion evaporation-mass spectrometry. *Int. J. Mass Spectrom. Ion Phys.* **1983**, *50* (3), 331–347.

[98] Iribarne, J. V.; Thomson, B. A. On the evaporation of small ions from charged droplets. *J. Chem. Phys.* **1976**, *64* (6), 2287–2294.

[99] Cech, N. B.; Enke, C. G. Relating electrospray ionization response to nonpolar character of small peptides. *Anal. Chem.* **2000**, *72* (13), 2717–2723.

[100] Shimbo, K.; Oonuki, T.; Yahashi, A.; Hirayama, K.; Miyano, H. Precolumn derivatization reagents for high-speed analysis of amines and amino acids in biological fluid using liquid chromatography/electrospray ionization tandem mass spectrometry. *Rapid Commun. Mass Spectrom.* **2009**, *23* (10), 1483–1492.

[101] Pashkova, A.; Moskovets, E.; Karger, B. L. Coumarin tags for improved analysis of peptides by MALDI-TOF MS and MS/MS. 1.

Enhancement in MALDI MS signal intensities. *Anal. Chem.* **2004**, *76* (15), 4550–4557.

[102] Cech, N. B.; Krone, J. R.; Enke, C. G. Predicting electrospray response from chromatographic retention time. *Anal. Chem.* **2001**, *73* (2), 208–213.

[103] Liigand, P.; Kaupmees, K.; Kruve, A. Influence of the amino acid composition on the ionization efficiencies of small peptides. *J. Mass Spectrom.* **2019**, *54* (6), 481–487.

[104] Rebane, R.; Oldekop, M. L.; Herodes, K. Comparison of amino acid derivatization reagents for LC-ESI-MS analysis. Introducing a novel phosphazene-based derivatization reagent. *J. Chromatogr. B Anal. Technol. Biomed. Life Sci.* **2012**, *904*, 99–106.

[105] Leng, J.; Wang, H.; Zhang, L.; Zhang, J.; Wang, H.; Guo, Y. A highly sensitive isotope-coded derivatization method and its application for the mass spectrometric analysis of analytes containing the carboxyl group. *Anal. Chim. Acta* **2013**, *758*, 114–121.

[106] Mirzaei, H.; Regnier, F. Enhancing electrospray ionization efficiency of peptides by derivatization. *Anal. Chem.* **2006**, *78* (12), 4175–4183.

[107] Hermans, J.; Ongay, S.; Markov, V.; Bischoff, R. Physicochemical parameters affecting the electrospray ionization efficiency of amino acids after acylation. *Anal. Chem.* **2017**, *89* (17), 9159–9166.

[108] Connolly, M. L. Analytical molecular surface calculation. *J. Appl. Crystallogr.* **1983**, *16* (5), 548–558.

[109] Raji, M. A.; Fryčák, P.; Temiyasathit, C.; Kim, S. B.; Mavromaras, G.; Ahn, J. M.; Schug, K. A. Using multivariate statistical methods to model the electrospray ionization response of GXG tripeptides based on multiple physicochemical parameters. *Rapid Commun. Mass Spectrom.* **2009**, *23* (14), 2221–2232.

[110] Randall, S. M.; Koryakina, I.; Williams, G. J.; Muddiman, D. C. Evaluating nonpolar surface area and liquid chromatography/mass spectrometry response: An application for site occupancy measurements for enzyme intermediates in polyketide biosynthesis. *Rapid Commun. Mass Spectrom.* **2014**, *28* (23), 2511–2522.

[111] Toyo'oka, T. Derivatization-based high-throughput bioanalysis by LC-MS. *Anal. Sci.* **2017**, *33* (5), 555–564.

[112] Liigand, J.; Kruve, A.; Leito, I.; Girod, M.; Antoine, R. Effect of mobile phase on electrospray ionization efficiency. *J. Am. Soc. Mass Spectrom.* **2014**, *25* (11), 1853–1861.

[113] Roth, K. D. W.; Huang, Z. H.; Sadagopan, N.; Watson, J. T. Charge derivatization of peptides for analysis by mass spectrometry. *Mass Spectrom. Rev.* **1998**, *17* (4), 255–274.

[114] Li, X.; Franke, A. A. Improved LC-MS method for the determination of fatty acids in red blood cells by LC-Orbitrap MS. *Anal. Chem.* **2011**, *83* (8), 3192–3198.

[115] Kretschmer, A.; Giera, M.; Wijtmans, M.; De Vries, L.; Lingeman, H.; Irth, H.; Niessen, W. M. A. Derivatization of carboxylic acids with 4-APEBA for detection by positive-ion LC-ESI-MS(/MS) applied for the analysis of prostanoids and NSAID in urine. *J. Chromatogr. B Anal. Technol. Biomed. Life Sci.* **2011**, *879* (17–18), 1393–1401.

[116] Julka, S.; Regnier, F. E. Recent advancements in differential proteomics based on stable isotope coding. *Briefings Funct. Genomics Proteomics* **2005**, *4* (2), 158–177.

[117] Hong, S. M.; Tanaka, M.; Koyanagi, R.; Shen, W.; Matsui, T. Structural design of oligopeptides for intestinal transport model. *J. Agric. Food Chem.* **2016**, *64* (10), 2072–2079.

[118] Boersema, P. J.; Raijmakers, R.; Lemeer, S.; Mohammed, S.; Heck, A. J. R. Multiplex peptide stable isotope dimethyl labeling for quantitative proteomics. *Nat. Protoc.* **2009**, *4* (4), 484–494.

[119] Mochizuki, T.; Taniguchi, S.; Tsutsui, H.; Min, J. Z.; Inoue, K.; Todoroki, K.; Toyo'oka, T. Relative quantification of enantiomers of chiral amines by high-throughput LC-ESI-MS/MS using isotopic variants of light and heavy L-pyroglutamic acids as the derivatization reagents. *Anal. Chim. Acta* **2013**, *773*, 76–82.

[120] Piovesana, S.; Montone, C. M.; Cavaliere, C.; Crescenzi, C.; La Barbera, G.; Laganà, A.; Capriotti, A. L. Sensitive untargeted identification of short hydrophilic peptides by high performance liquid chromatography on porous graphitic carbon coupled to high resolution mass spectrometry. *J. Chromatogr. A* **2019**, *1590*, 73–79.

[121] Greguš, M.; Kostas, J. C.; Ray, S.; Abbatiello, S. E.; Ivanov, A. R. Improved sensitivity of ultralow flow LC-MS-based proteomic profiling of limited samples using monolithic capillary columns and FAIMS technology. *Anal. Chem.* **2020**, *92* (21), 14702–14712.

[122] Lortie, M.; Bark, S.; Blantz, R.; Hook, V. Detecting low-abundance vasoactive peptides in plasma: progress toward absolute quantitation

using nano liquid chromatography-mass spectrometry. *Anal. Biochem.* **2009**, *394* (2), 164–170.

[123] Glass, D. J. Skeletal muscle hypertrophy and atrophy signaling pathways. *Int. J. Biochem. Cell Biol.* **2005**, *37* (10), 1974–1984.

[124] Ikemoto, M.; Nikawa, T.; Takeda, S.; Watanabe, C.; Kitano, T.; Baldwin, K. M.; Izumi, R.; Nonaka, I.; Towatari, T.; Teshima, S.; Rokutan, K.; Kishi, K. Space shuttle flight (STS - 90) enhances degradation of rat myosin heavy chain in association with activation of ubiquitin-proteasome pathway. *FASEB J.* **2001**, *15* (7), 1279–1281.

[125] Hanh, V. T.; Shen, W.; Tanaka, M.; Siltari, A.; Korpela, R.; Matsui, T. Effect of aging on the absorption of small peptides in spontaneously hypertensive rats. *J. Agric. Food Chem.* **2017**, *65* (29), 5935–5943.

[126] Jappar, D.; Wu, S. P.; Hu, Y.; Smith, D. E. Significance and regional dependency of peptide transporter (PEPT) 1 in the intestinal permeability of glycylsarcosine: *In situ* single-pass perfusion studies in wild-type and *Pept1* knockout mice. *Drug Metab. Dispos.* **2010**, *38* (10), 1740–1746.

[127] Madara, J. L.; Barenberg, D.; Carlson, S. Effects of cytochalasin D on occluding junctions of intestinal absorptive cells: Further evidence that the cytoskeleton may influence paracellular permeability and junctional charge selectivity. *J. Cell Biol.* **1986**, *102* (6), 2125–2136.

[128] Hong, S. M.; Tanaka, M.; Yoshii, S.; Mine, Y.; Matsui, T. Enhanced visualization of small peptides absorbed in rat small intestine by phytic-acid-aided matrix-assisted laser desorption/ionization-imaging mass spectrometry. *Anal. Chem.* **2013**, *85* (21), 10033–10039.

[129] Aito-Inoue, M.; Lackeyram, D.; Fan, M. Z.; Sato, K.; Mine, Y. Transport of a tripeptide, Gly-Pro-Hyp, across the porcine intestinal brush-border membrane. *J. Pept. Sci.* **2007**, *13* (7), 468–474.

[130] Dörfel, M. J.; Huber, O. Modulation of tight junction structure and function by kinases and phosphatases targeting occludin. *J. Biomed. Biotechnol.* **2012**, *2012*, 807356.

[131] Estaki, M. Interplay between intestinal alkaline phosphatase, diet, gut microbes and immunity. *World J. Gastroenterol.* **2014**, *20* (42), 15650.

[132] Brodin, B.; Nielsen, C. U.; Steffansen, B.; Frøkjær, S. Transport of peptidomimetic drugs by the intestinal di/tri-peptide transporter, PepT1. *Pharmacol. Toxicol.* **2002**, *90* (6), 285–296.

[133] Newstead, S.; Drew, D.; Cameron, A. D.; Postis, V. L. G.; Xia, X.; Fowler, P. W.; Ingram, J. C.; Carpenter, E. P.; Sansom, M. S. P.; McPherson, M. J.; Baldwin, S. A.; Iwata, S. Crystal structure of a prokaryotic homologue of the mammalian oligopeptide-proton symporters, PepT1 and PepT2. *EMBO J.* **2011**, *30* (2), 417–426.

[134] Chothe, P.; Singh, N.; Ganapathy, V. Evidence for two different broad-specificity oligopeptide transporters in intestinal cell line Caco-2 and colonic cell line CCD841. *Am. J. Physiol. - Cell Physiol.* **2011**, *300* (6), 1260–1269.

[135] Xu, Q.; Hong, H.; Wu, J.; Yan, X. Bioavailability of bioactive peptides derived from food proteins across the intestinal epithelial membrane: A review. *Trends Food Sci. Technol.* **2019**, *86* (February), 399–411.

[136] Sánchez-Rivera, L.; Ares, I.; Miralles, B.; Gómez-Ruiz, J. Á.; Recio, I.; Martínez-Larrañaga, M. R.; Anadón, A.; Martínez, M. A. Bioavailability and kinetics of the antihypertensive casein-derived

peptide HLPLP in rats. *J. Agric. Food Chem.* **2014**, *62* (49), 11869–11875.

[137] Picariello, G.; Ferranti, P.; Addeo, F. Use of brush border membrane vesicles to simulate the human intestinal digestion. *Food Res. Int.* **2016**, *88* (Part B), 327–335.

[138] Abe, T.; Kohno, S.; Yama, T.; Ochi, A.; Suto, T.; Hirasaka, K.; Ohno, A.; Teshima-Kondo, S.; Okumura, Y.; Oarada, M.; Choi, I.; Mukai, R.; Terao, J.; Nikawa, T. Soy glycinin contains a functional inhibitory sequence against muscle-atrophy-associated ubiquitin ligase Cbl-b. *Int. J. Endocrinol.* **2013**, *2013*, 907565.

[139] Ohno, A.; Ochi, A.; Maita, N.; Ueji, T.; Bando, A.; Nakao, R.; Hirasaka, K.; Abe, T.; Teshima-Kondo, S.; Nemoto, H.; Okumura, Y.; Higashibata, A.; Yano, S.; Tochio, H.; Nikawa, T. Structural analysis of the TKB domain of ubiquitin ligase Cbl-b complexed with its small inhibitory peptide, Cblin. *Arch. Biochem. Biophys.* **2016**, *594*, 1–7.

[140] Ten Have, G. A. M.; Van Der Pijl, P. C.; Kies, A. K.; Deutz, N. E. P. Enhanced lacto-tri-peptide bio-availability by co-ingestion of macronutrients. *PLoS One* **2015**, *10* (6), e0130638.

[141] Pye, C. R.; Hewitt, W. M.; Schwochert, J.; Haddad, T. D.; Townsend, C. E.; Etienne, L.; Lao, Y.; Limberakis, C.; Furukawa, A.; Mathiowetz, A. M.; Price, D. A.; Liras, S.; Lokey, R. S. Nonclassical size dependence of permeation defines bounds for passive adsorption of large drug molecules. *J. Med. Chem.* **2017**, *60* (5), 1665–1672.

Acknowledgements

I would like to take this opportunity to express my gratitude to all the people who helped me to finish my doctoral dissertation. First and foremost, I would like to thank my supervisor, Prof. Toshiro Matsui, for his guidance and support during my study. His enthusiasm and strict requirement for high-quality research work has left a deep impression on me. His knowledge and expert academic advice have been indispensable for me to accomplish this work. I would also like to thank the rest of my thesis committee, Prof. Mitsuhiro Furuse and Assoc. Prof. Mitsuru Tanaka, for their professional review and valuable comments on my doctoral dissertation.

I am grateful for Japan Society for the Promotion of Science (JSPS) for the financial support during my Ph.D. study. This work was supported by JSPS Research Fellowship for Young Scientists grant (No. 19J20948).

I would like to thank Prof. Takeshi Nikawa from Department of Nutritional Physiology, Institute of Biomedical Sciences, Graduate School,

Tokushima University for the opportunity of collaborative study on Cblin pentapeptides.

I would like to thank Assoc. Prof. Mitsuru Tanaka. His infinite enthusiasm and passion always motivated me all the way through my study. Special thanks to Ms. Kaori Miyazaki for taking care of all official matters so that I could focus on my research.

I would like to thank all members of Lab. Food Analysis. Special thanks to Riho Koyanagi for her guidance and support, to my partners Mika Kojima and Kiyomi Ono for their scientific support and encouragement. Many thanks to Toshihiko Fukuda, Si Jing Chen for the inspiration and support, to Genki Komabayashi, Satoshi Tajiri, Junji Tabata, Yusuke Terazono, Naoki Morishita, and Risa Yoshida for the friendship and encouragement. I would also like to express my heart-felt gratitude to all other members for their kindness. The stay in Lab. Food Analysis has become an invaluable journey for me thanks to you all.

Last but not least, I would like to thank my parents, Liang Shen and Mei Guo, who valued knowledge, devoted themselves into the education of me and my brother, and encouraged me to go see the bigger world.